Implementation of the biogenic emission model MEGAN(v2.1) into the ECHAM6-HAMMOZ chemistry climate model.

Alexandra-Jane Henrot [1,2], Tanja Stanelle [3], Sabine Schröder [1], Colombe Siegenthaler [4], Domenico Taraborrelli [1], and Martin G. Schultz [1]

[1]Forschungszentrum Jülich GmbH, IEK-8:Troposphere, Jülich, Germany.
[2]Unité de Modélisation du Climat et des Cycles Biogéochimiques, University of Liège, Liège, Belgium.
[3]ETH Zurich, Institute for Atmospheric and Climate Science, Zurich, Switzerland.
[4]ETH Zurich, Center for Climate System Modelling, Zurich, Switzerland.

Correspondence to: Alexandra-Jane Henrot (alexandra.henrot@ulg.ac.be)

Abstract. A biogenic emission scheme based on the Model of Emissions of Gases and Aerosols from Nature (MEGAN) version 2.1 (Guenther et al., 2012) has been integrated into the ECHAM6-HAMMOZ chemistry climate model in order to calculate the emissions from terrestrial vegetation of 32 compounds. The estimated annual global total for the reference simulation is 634 Tg C yr^{-1} (simulation period 2000-2012). Isoprene is the main contributor to the average emission total accounting for 66 % (417 Tg C yr^{-1}), followed by several monoterpenes (12 %), methanol (7 %), acetone (3.6 %) and ethene (3.6 %). Regionally, most of the high annual emissions are found to be associated to tropical regions and tropical vegetation types.

In order to evaluate the implementation of the biogenic model in ECHAM-HAMMOZ, global and regional BVOC emissions of the reference simulation were compared to previous published experiment results with the MEGAN model. Several sensitivity simulations were performed to study the impact of different model input and parameters related to the vegetation cover and the ECHAM6 climate. BVOC emissions obtained here are within the range of previous published estimates. The large range of emission estimates can be attributed to the use of different input data and empirical coefficients within different setups of the MEGAN model. The biogenic model shows a high sensitivity to the changes in plant functional type (PFT) distributions and associated emission factors for most of compounds. The global emission impact for isoprene is about -9 %, but reaches +75 % for α-pinene when switching from global emission factor maps to PFT-specific emission factor distributions. The highest sensitivity of isoprene emissions is calculated when considering soil moisture impact, with a global decrease of 12.5 % when the soil moisture activity factor is included in the model parameterization. Nudging ECHAM6 climate towards ERA-Interim reanalysis has impact on the biogenic emissions, slightly lowering the global total emissions and their interannual variability.

1 Introduction

The majority of volatile organic compounds emitted from the terrestrial biosphere (BVOCs), including hydrocarbons (isoprene, monoterpenes, and sesquiterpenes) as well as oxygenated organic compounds, are highly reactive and have been shown to affect both gas phase and heterogeneous atmospheric chemistry at local and global scales (Ashworth et al., 2013). Photo-oxidation of BVOCs notably, in the presence of nitrogen oxides (NOx), contributes to the formation of carbon monoxide (CO), hydroxyl

radical (OH) and tropospheric ozone (Pfister et al., 2008; Granier et al., 2000), thus influencing the oxidative capacity of the atmosphere (Atkinson and Arey, 2003; Pacifico et al., 2009; Taraborrelli et al., 2012), and leads to secondary organic aerosol (SOA) particle formation (Hallquist et al., 2009; van Donkelaar et al., 2007). Through their effects on atmospheric chemistry, aerosol concentrations, and the global carbon cycle, BVOC emissions also influence global climate (Constable et al., 1999;

5 Collins et al., 2002). Terrestrial vegetation is thought to account for around 90 % of the total of non-methane VOCs emitted into the atmosphere each year (Guenther et al., 1995). Isoprene is quantitatively the most important of the BVOCs, with an estimated global annual emission of about 400-600 Tg of carbon (Arneth et al., 2011; Guenther et al., 2012).

BVOCs are therefore a crucial component of the Earth system that has to be considered in global and regional chemical transport models. Quantitative estimates of their emissions into the atmosphere are needed for numerical assessments of their

10 impacts on past, present and future air quality and climate (Sindelarova et al., 2014). BVOC emission strengths vary by plant species and depend on biological parameters (e. g. water stress) (Pfister et al., 2008; Pegoraro et al., 2004), physical conditions (e. g. temperature, radiation) (Guenther et al., 1995; Li and Sharkey, 2013), and chemical variables (e. g. tropospheric ozone, carbon dioxide) (Velikova et al., 2005; Rosenstiel et al., 2003). Several models have been developed for estimation of BVOC emissions from vegetation (Pierce and Waldruff, 1991; Guenther et al., 1995; Niinemets et al., 1999; Martin et al., 2000; Arneth

15 et al., 2007).

The biogenic emission model used in the present study is based on the MEGAN model (Guenther et al., 1995, 2006, 2012). The current version of MEGAN, MEGANv2.1 (Guenther et al., 2012), simulates the fluxes of 20 classes of BVOCs which are then decomposed into 150 individual species, including isoprene, monoterpenes, sesquiterpenes, and other oxygenated volatile organic compounds. During the past ten years, MEGAN has been widely used within the scientific community for the

20 estimation of BVOC emissions as an offline model (Guenther et al., 2006, 2012; Müller et al., 2008; Sindelarova et al., 2014; Messina et al., 2015) and has been incorporated into various earth system and chemistry transport models (Guenther et al., 2006, 2012; Heald et al., 2008; Pfister et al., 2008; Stavrakou et al., 2009; Emmons et al., 2010; Tilmes et al., 2015; Messina et al., 2015).

In this study, we have implemented the MEGANv2.1 model into the ECHAM6-HAMMOZ chemistry climate model. The

25 aim of the present study is (i) to present the updated version of the biogenic emission module implemented into ECHAM6-HAMMOZ, (ii) to evaluate present-day global and regional scale emissions for a series of 32 compounds, (iii) to compare MEGAN-ECHAM-HAMMOZ basic results to previous offline and online experiment results with the MEGAN model and (iv) to test the sensitivity of BVOC emissions to climate and vegetation dependent model parameters.

2 Model description

30 2.1 Atmospheric model ECHAM-HAMMOZ

ECHAM-HAMMOZ is a comprehensive chemistry climate model that describes aerosol and gas-phase chemical processes in the troposphere and stratosphere including their coupling via heterogeneous reactions and oxidation of aerosol precursors. ECHAM-HAMMOZ is developed by a consortium composed of ETH Zurich (Switzerland), Max Planck Institute for Me-

teorology (Germany), Forschungszentrum Jülich (Germany), University of Oxford (UK), Institut für Troposphärenforschung (Germany) and the Finnish Meteorological Institute (Finland). We used here the most recent version ECHAM6.3.00-HAM2.3-MOZ1.0(rc2). The model is based on the ECHAM6 atmospheric general circulation model (Roeckner et al., 2003; Stevens et al., 2013), including the phenology model JSBACH (Raddatz et al., 2007; Brovkin et al., 2009), the HAM aerosol model (Stier et al., 2005; Zhang et al., 2012), and a chemistry module derived from the MOZART chemistry transport model (Emmons et al., 2010; Lamarque et al., 2012). For the simulations of this study, ECHAM6-HAMMOZ is employed in its stand-alone atmospheric GCM mode, i.e. without interactive aerosol and chemistry. Thus, we basically run the ECHAM6 GCM with the MEGAN emissions module as the sole chemistry component. ECHAM6 dynamics (vorticity and divergence of the wind field, temperature and surface pressure) are calculated in spectral space with triangular truncation at term 63 (T63), while physics are calculated on a 1.8° x 1.8° Gaussian grid (Roeckner et al., 2003). The simulations use 47 vertical levels, from the surface to 0.01 hPa, and a time step of 7.5 minutes. Sea-surface temperatures and sea-ice coverage are prescribed for each year of simulation, following the Coupled Model Intercomparison Project Phase 5 (CMIP5) AMIP-simulation protocol (Giorgetta et al., 2012). The gas climatologies of CO_2, CH_4, N_2O, and chloroflourocarbons (CFCs) are specified by a single value meant to be representative for the tropospheric concentration of each year of simulation. For several sensitivity simulations, ECHAM6 is run in nudged mode, constraining large-scale meteorology by the ECMWF ERA-Interim meteorological fields (Dee et al., 2011). The nudging tendency is applied after model dynamics, in spectral space. The nudging time scales are 6h for vorticity, 48h for divergence, 24h for temperature, and 24h for surface pressure (Lohmann and Hoose, 2009; Zhang et al., 2014).

2.2 Land surface model JSBACH

JSBACH is a state-of-the art Earth System Model land surface scheme that simulates fluxes of energy, water, momentum, and CO_2 between land and atmosphere, including interactive and dynamic vegetation (Raddatz et al., 2007; Brovkin et al., 2009). The modeling concept of JSBACH is based on a tiled (fractional) structure of the land surface. Each land grid cell is divided into tiles covered with a variable number of Plant Functional Types (PFTs), bare surface, and tiles with land cover excluded from natural vegetation dynamics (Reick et al., 2013). The soil hydrology and temperatures are modeled by a five-layer scheme (Hagemann and Stacke, 2015). The dynamic vegetation component, simulating natural changes in biogeography on the basis of competition between PFTs (Reick et al., 2013), has not been activated in this study. The spatial distribution of the PFTs is prescribed on the basis of global potential land cover maps (Pongratz et al., 2008). For the present study, we used JSBACH with 11 PFTs, as fixed for the CMIP5 simulation protocol (Reick et al., 2013; Brovkin et al., 2013).

2.3 Biogenic emission module MEGAN

Emissions of biogenic compounds from terrestrial vegetation are estimated using the Model of Emissions of Gases and Aerosols from Nature MEGAN (Guenther et al., 1995, 2006, 2012). The current version of the model, MEGANv2.1 (Guenther et al., 2012), calculates the net primary emission of 20 compound classes, which are then decomposed into 150 individual species such as isoprene, monoterpenes, sesquiterpenes, carbon monoxide, alkanes, alkenes, aldehydes, acids, ketones and other oxygenated VOCs. The net emission rate (in units of μg compound grid cell^{-1} h^{-1}) of each compound into the above-canopy

atmosphere from a model grid cell is calculated according to:

$$Emission(i) = EF(i) \cdot \gamma \cdot S \tag{1}$$

where $EF(i)$ (μg m^{-2} h^{-1}) is the emission potential (also named emission factor) of a compound i at standard conditions of light and temperature (i. e. photosynthetic photon flux density of 1000 μmol m^{-2} s^{-1} and leaf temperature of 30°C), γ is the dimensionless emission activity factor that accounts for emission response to meteorological and phenological conditions, and S (m^2) is the grid cell area.

The biogenic emission module implemented into ECHAM6-HAMMOZ is adapted from MEGANv2.1. It includes 32 compounds grouped into 17 classes (see Table 1).

2.3.1 Emission activity factor γ

The emission activity factor γ for each compound is calculated following the MEGANv2.1 parameterization (Guenther et al., 2012):

$$\gamma = \gamma_{CE} \cdot \gamma_A \cdot \gamma_{SM} \cdot \gamma_{CO2}. \tag{2}$$

γ_{CE} accounts for variations associated with Leaf Area Index (LAI) (m^2 m^{-2}), Photosynthetic Photon Flux Density (PPFD) (μmol of photons in 400-700 nm range m^{-2} s^{-1}) and temperature (K). The basic equation used in the fortran code of MEGANv2.1 to calculate γ_{CE} is:

$$\gamma_{CE} = \gamma_{LAI} \cdot (1 - LDF) \cdot \gamma_{TLI} + C_{CE} \cdot LAI \cdot LDF \cdot \gamma_{TLD} \tag{3}$$

where C_{CE} is the canopy environment coefficient (assigned a value that results in $\gamma = 1$ for the standard conditions), and γ_{LAI}, γ_{TLI} and γ_{TLD} are the activity factors for LAI, light and temperature. Different expressions for the activity factor for temperature are considered for light-dependent (γ_{TLD}) and light-independent (γ_{TLI}) emissions using the light dependence fraction LDF specific for each compound (Guenther et al., 2012). Light-dependent emissions are calculated following the isoprene-response to temperature described by Guenther et al. (2006). Light-independent emissions follow the monoterpene exponential temperature response described by Guenther et al. (1993). In order to avoid the use of a detailed canopy environment model calculating light and temperature at each canopy depth, we applied the Parameterised Canopy Environment Emission Activity (PCEEA) approach (Guenther et al., 2006). The calculation of the light-dependent activity factor with a detailed canopy environment model (i. e. $C_{CE} \cdot LAI \cdot \gamma_{TLD}$) is replaced by a parameterized canopy environment activity factor (i. e. $\gamma_{LAI} \cdot \gamma_P \cdot \gamma_T$) as described in Guenther et al. (2006). We refer the reader to the description of Guenther et al. (2006, 2012) for the details of the LAI and light-dependent activity factor computations. With this approach, both light-dependent and light-independent factors are multiplied by the LAI activity factor and are thus not directly proportional to the LAI. On this point, the algorithm applied here differs from the MEGAN activity factor algorithm as described in Eq. (2) in Guenther et al. (2012). The light-independent activity factor γ_{TLI} is calculated here assuming that leaf temperature is equal to ambient air

temperature. In the absence of a detailed canopy model, we do not distinguish between sunlit and shaded leaves that can show significant temperature differences. Leaves in direct sunlight often experience temperatures that are a degree or more higher than ambient air while shaded leaves are often cooler than ambient air temperature (Guenther et al., 2012). This simplification can lead to a small underestimation ($< 5\%$) of light-independent BVOC emissions as reported in Guenther et al. (2012). Detailed formula and parameters per compound class are given in Supplementary Material (Sect. S1 and S2). The equation for γ_{CE} applied here is thus:

$$\gamma_{CE} = \gamma_{LAI} \cdot ((1 - LDF) \cdot \gamma_{TLI} + LDF \cdot \gamma_P \cdot \gamma_T). \tag{4}$$

The activity factors are calculated on the basis of the leaf area index, the lowest atmospheric model level temperature and surface photosynthetically active radiation at each time step in the ECHAM6-HAMMOZ model, as well as the average temperature and radiation conditions over the last 24 hours. The leaf area index is calculated at each model time step in JSBACH taking into account a full plant phenology scheme, and is averaged over the vegetated part of the grid cell to be used in the biogenic emission module. Variations of the biomass calculated by the vegetation model JSBACH are taken into account for the biogenic emissions via the corresponding changes in LAI.

The γ_A factor represents the leaf age emission activity factor. Its calculation is based on a decomposition of the canopy into fractions of new, growing, mature and old foliage derived from the current and previous month LAI, following the parameterization described by Guenther et al. (2006, 2012). The γ_{SM} and γ_{CO2} factors account for the dependence of isoprene emission on respectively the soil moisture and the atmospheric concentration of CO_2 as described by Guenther et al. (2012). For compounds other than isoprene, γ_{SM} and γ_{CO2} equal 1. The soil water activity factor is evaluated using the relative soil water amount calculated with the soil water model included in ECHAM6 (Hagemann and Stacke, 2015). The atmospheric CO_2 concentration is prescribed annually, using a global value from the Representative Concentration Pathway scenario RCP 4.5 (stabilization scenario where total radiative forcing is stabilized before 2100 (Thomson et al., 2011). By default, γ_{SM} and γ_{CO2} are not activated, and set equal to 1 for isoprene.

2.3.2 Emission factor EF

Emission factor EF for each compound can be specified from global gridded potential emission maps based on species composition and species-specific emission factors compiled from detailed land cover and plant species distributions (Guenther et al., 2012). Emission factors from global maps are available from the original MEGANv2.1 code for 10 predominant compounds, i. e. isoprene, α-pinene, β-pinene, 3-carene, limonene, myrcene, t-β-ocimene, sabinene, 232-MBO and nitric oxide. Another option to obtain the emission factor for each compound is to use plant functional types (PFT) distributions and PFT specific emission potentials (Guenther et al., 2012). The emission factor of a grid cell for each compound is calculated as:

$$EF(i) = \sum \epsilon(i,j) \cdot PFT_j \tag{5}$$

where $\epsilon(i,j)$ is the emission factor of compound i at standard conditions of light and temperature for the plant functional type j (constant in time and space), and PFT_j is the fraction of the grid cell covered by the PFT j. MEGANv2.1 includes a 15-PFT

distribution derived from the PFT scheme of the Community Land Model version 4 CLM4 (Lawrence et al., 2011), related to the year 2000 and based on Moderate Resolution Imaging Spectroradiometer (MODIS) land surface datasets (Lawrence and Chase, 2007) and a crop dataset (Ramankutty et al., 2008). Specific emission factors for each compound attributed to the 15 PFTs can be found in Table S2 of Supplementary Material. By default, the biogenic emission module runs with the emission factors from global maps for the 10 compounds listed above and calculates the emission factors from the PFT specific values and fractions for the other modelled compounds. Maps of emission factors as well as PFT fractions have been interpolated from their original resolution (0.5 x 0.5) in the current resolution of the ECHAM-HAMMOZ model (T63).

We have introduced in the biogenic emission module the possibility to replace the MEGAN2.1-CLM4 PFT distribution by the PFT distribution of the JSBACH model. In order to have a sufficiently detailed PFT classification to take into account the variability in PFT specific emission factors, the JSBACH 11 PFT-classification is extended to 14 PFTs to be as close as possible to the MEGAN2.1-CLM4 15-PFT classification. The correspondence between both PFT classifications is given in Table 2.

The extra-tropical tree types of the JSBACH 11 PFT-classification (i.e. extra-tropical evergreen (type 3) and extra-tropical deciduous (type 4)), as well as the C3 grass type are subdivided in order to make a distinction between broadleaf and needleleaf trees and temperate and boreal types. Fractions of broadleaf and needleleaf trees are derived from natural vegetation distributions (Pongratz et al., 2008, 2009), reconstructed from the global potential vegetation maps of Ramankutty and Foley (1999).

The separation between boreal and temperate trees, as well as cold and cool C3 grasses is based on bioclimatic limits taken from Sitch et al. (2003) for trees, and from Oleson et al. (2010), based on Levis et al. (2004), for C3 grasses. Tree types are classified as boreal if the temperature of the coldest month (calculated from a 20-year run over the period 1990-2009 with the ECHAM6 model) is below -2°C. C3 grasses are classified as cold or arctic (using the denomination of the MEGAN2.1-CLM4 PFT classification) if the temperature of the coldest month lies below -17°C.

Tropical tree types (PFTs 1 and 2 in JSBACH) are not subdivided as their correspondence to MEGAN2.1-CLM4 tropical PFTs is straightforward. JSBACH shrub PFTs represent deciduous shrubs in warm/temperate and cold/boreal environments, and directly correspond to the shrub types of the MEGAN2.1-CLM4 classification. No evergreen shrub type is considered in JSBACH. In consequence, the broadleaf evergreen temperate shrub type (PFT 9) of the MEGAN2.1-CLM4 classification has no correspondance in the extended JSBACH classification. Finally, as MEGAN2.1-CLM4 PFT classification does not distinguish grasses and pastures, these two types are clustered in the extended JSBACH classification.

The PFT correspondence applied here enables the use of MEGAN2.1 PFT specific emission factors, calculated from global averages of species-specific emission factors from more than 2000 different ecoregions (Guenther et al., 2012). The extended JSBACH-PFT classification is only used here in the biogenic emission module for the calculation of emission factors, and does not impact the calculation in the JSBACH model of the PFT fractions and of the LAI, based on the original 11-PFTs specific parameters.

3 Simulation design

In order to evaluate the implementation of MEGAN in ECHAM-HAMMOZ and its sensitivity to different model settings, we have performed several simulations at the global scale at a T63 spatial resolution (listed in Table 3). All simulations have been run for 12 years for the period 2000-2012, starting from a one-year spin-up with ECHAM-HAMMOZ. For the reference simulation (CTRL), the biogenic emission module is run with the emission factors from global maps for 10 compounds (isoprene, α-pinene, β-pinene, 3-carene, limonene, myrcene, t-β-ocimene, sabinene, 232-MBO and nitric oxide) and with MEGAN2.1-CLM4 PFT-specific emission factors for the rest of the compounds. In the first sensitivity simulations, we evaluate the impact of PFT distributions on the modeled emissions, by using the PFT-specific emission factors calculated from the PFT fractions taken from the MEGAN2.1-CLM4 (experiment PFT-CLM4) and the extended-JSBACH PFT (experiment PFT-JSBACH) distributions, respectively. In experiment TEST-SM, the impact of soil moisture on isoprene emissions is analysed, by activating the soil moisture activity factor. The effect of a constrained meteorology on the emissions simulated with the biogenic module are evaluated in the last experiments TEST-NUDG and TEST-NUDG+SM.

4 Biogenic emission model results

4.1 Reference simulation

The biogenic module monthly outputs have been averaged over the 2000-2012 period to calculate the global annual emission totals of the 32 compounds for the reference simulation (see Table 4). The global annual emission total for the averaged period reaches 634.1 ± 12.5 Tg C yr^{-1}. Isoprene is the most emitted compound with a global annual emission of 417 ± 10.2 Tg C yr^{-1} (473 Tg (species) yr^{-1}), accounting for 65.8 % of the total BVOC emissions. Monoterpene global annual emission (considering only the sum of α-pinene, β-pinene, limonene, sabinene, myrcene, 3-carene and t-β-ocimene emissions) is 78.3 ± 1.2 Tg C yr^{-1} (88.8 Tg (species) yr^{-1}) and contributes to 12.3 % of the total BVOC emission. Among the monoterpenes, α-pinene is the most abundant compound, followed by β-pinene and t-β-ocimene. Following the monoterpenes, methanol, acetone and ethene are the most emitted compounds with respectively 43.9 ± 0.5, 22.9 ± 0.3 and 22.9 ± 0.4 Tg C yr^{-1}, contributing to 6.9, 3.6 and 3.6 % of the total emission. The carbon monoxide global annual emission is 41.1 ± 0.6 Tg C yr^{-1}.

Annual emissions of the five most emitted compounds and β-caryophyllene for seven regions of the world are presented in Fig. 1. Regions have been defined following the protocol of the GlobEmission project (http://www.globemission.eu), except that African regions have been grouped into one. All compounds are mainly emitted in southern and tropical regions with a dominance of South America, followed by Africa, South Asia and Australia. In the Northern Hemisphere, emissions mainly come from North America, followed by Russia and Europe.

Global, Northern and Southern Hemisphere monthly mean emissions for the six compounds averaged over the reference simulation period are presented in Fig. 2. The maximum global emission occurs in July for most of compounds and emissions are generally higher during the Northern Hemisphere summer. Regions of the Northern Hemisphere are minor contributors to the global annual total emissions, but seasonal emissions fluctuations in the Northern Hemisphere are the main driver for the

global seasonal emission profile. Isoprene shows a more constant seasonal cycle, due to the fact that it is mainly emitted by tropical regions with opposite seasonal cycles, thus compensating in the global annual mean.

Spatial distributions of the main compound emissions for the Northern Hemisphere summer (June-July-August emission mean) and winter (December-January-February emission mean) are shown in Fig. 3 and Fig. 4. As observed in the global regional means (Fig. 1), emissions are generally higher in tropical regions, especially South America, Africa and Indonesia and are lower at middle and high latitudes. Tropical regions are high emitters due to the year-long warm temperatures and high incoming radiation, together with high biomass density and emission factors associated to tropical vegetation types. In the temperate and high latitude zones dominated by deciduous and coniferous forests, emissions vary over the seasons by several orders of magnitude due to seasonal fluctuations in temperature, solar radiation and loss of biomass inducing LAI changes. The summer-winter contrast in the Northern Hemisphere emissions is particularly marked for monoterpenes and methanol, for which temperate and coniferous vegetation types have high emission factors.

4.2 Comparison to previous emission totals calculated with the MEGAN model

In order to evaluate the basic results of the biogenic emission module in ECHAM-HAMMOZ, we compare the global and regional total emissions of the reference simulation with emission totals obtained from previous published experiments with the MEGAN model (listed in Table 5). The annual global isoprene emission in our reference simulation of 417 Tg C year^{-1} is within the range of previous reported values calculated with different versions of the MEGAN models, varying between 361 and 601 Tg C year^{-1}. It is slightly less than previous estimates with different configurations of MEGANv2.1. (Messina et al., 2015; Sindelarova et al., 2014; Guenther et al., 2012). The annual global emission of monoterpenes is in general lower than reported estimates with MEGANv2.1, but closer to previous emission totals with MEGANv2 (O'Donnell et al., 2011; Emmons et al., 2010). It should be noticed that differences in monoterpenes global emissions may be due to the consideration of different species in the global totals. Here, we simulate the emissions of seven monoterpenes, i.e. α-pinene, β-pinene, limonene, sabinene, myrcene, 3-carene and t-β-ocimene emissions. Methanol and acetone emissions, as well as the rest of the compound emission totals presented in Table 5, are in the middle of the ranges of previous emission estimates. Ethene total emission is similar to the total reported in Guenther et al. (2012), but β-caryophyllene total emission is lower. Similarly to Sindelarova et al. (2014) we estimate a global biogenic emission of 1.4 Tg C year^{-1} of toluene, being 18 % of the total estimated anthropogenic emissions 7.6 Tg C year^{-1} from the EDGAR database (Crippa et al., 2016). Misztal et al. (2015) estimate a maximum biogenic source of 5.5 Tg C year^{-1}. Such a biogenic source would reduce the underestimate of toluene by atmospheric models (Cabrera-Perez et al., 2016).

Many factors can explain the discrepancies between the reference simulation results of the present study and previous reported global estimates with the MEGAN model. First, each study uses its own set of input data (temperature, radiation, LAI, land cover, etc), derived from atmospheric model outputs or reanalysis data. Time periods of the simulations also cover different years, from one single-year (Millet et al., 2010; Guenther et al., 2012) to several decades (Arneth et al., 2011; Sindelarova et al., 2014). As already pointed out by Arneth et al. (2011), and confirmed by the estimations of Messina et al. (2015); Sindelarova et al. (2014), different meteorological forcings can lead to significant differences in emission estimates, e. g. more than 10

% difference in isoprene total emission using MEGANv2 (Guenther et al., 2006; Arneth et al., 2011). Furthermore, spatial resolutions of models and meteorological inputs vary over a large range, e. g. from a coarse resolution of 2.8° x 2.8° (Emmons et al., 2010) to a finer resolution of 0.5° x 0.5° (Guenther et al., 2012). The resolution effect can influence the total global emissions by a few percent, but can be more important if associated with coarse resolution land cover data (Pugh et al., 2013).

5   BVOC emissions are also very sensitive to changes in land cover and LAI inputs. Global isoprene emission sensitivity to differences in LAI varies from less than 10 % in MEGANv2.1 (Sindelarova et al., 2014; Messina et al., 2015) to about 30 % in MEGANv2 (Pfister et al., 2008; Guenther et al., 2012), depending on the LAI dataset considered. Messina et al. (2016) report a much lower sensitivity of other BVOC global emissions to LAI in MEGANv2.1 due to the specific light independent emission parameterization of the MEGAN model, but a significant response of the seasonal cycle of emissions to LAI changes. Changing

10   the land cover or PFT distributions and emission factors results in a wide range of BVOC estimates. Pfister et al. (2008) find a difference of 24 % in isoprene global emission by changing PFT distributions in MEGANv2. Sindelarova et al. (2014) and Messina et al. (2015) investigated the sensitivity of isoprene emission in MEGANv2.1 to different values of emission factors. The sensitivity of BVOC emissions to various PFT distributions and emission factors is addressed in the next section.

    The use of different versions of the MEGAN model in the listed studies, with different parameterizations and empirical

15   coefficients, can also result in differences in the global emission totals (Arneth et al., 2011). The introduction of light-dependent factors for other compounds than isoprene in MEGANv2.1 has notably a significant effect on global emissions (Messina et al., 2015). Moreover, a large range of variation of light-dependent emissions, especially for monoterpenes, is observed across plant species (Rinne, 2016). Thus, the use of a single LDF value per compound in MEGANv2.1 can introduce further uncertainties in the model emission estimates and discrepancies between model versions using different values of LDF. In the biogenic module

20   applied here the light-dependent activity factors are calculated using the Parameterized Canopy Environment Emission Activity (PCEEA) approach. This bulk canopy temperature parameterization is similar to the leaf-level temperature parameterization of the explicit canopy model but is slightly less sensitive to temperature. Guenther et al. (2006) report estimates of annual global isoprene emissions with the PCEEA approach that are within 5% of the value estimated using the standard MEGAN canopy environment model, but differences can be up to 25% for estimates at specific times and locations. The activation of

25   the CO_2 and soil moisture activity factors in MEGANv2.1 also impact isoprene global emissions. Taking into account the soil moisture effect decreases the global annual isoprene emission, by 7 % (Guenther et al., 2012) to 50 % (Sindelarova et al., 2014) depending on the soil moisture database. Similarly to Sindelarova et al. (2014), we have not activated the soil moisture factor for the reference simulation. Its impact on isoprene emission is described in the next section. When activated, the CO_2 activity factor leads to a slight increase of global isoprene emission by about 3 % for present-day CO_2 levels (Heald et al.,

30   2009; Sindelarova et al., 2014). The CO_2 activity factor is normalized to 1 for an ambient CO_2 concentration of 400 ppmv and decreases non-linearly if CO_2 concentration increases (Heald et al., 2009). Thus, it has only a slight impact on present-day isoprene emission, but it has to be taken into account for future simulations with CO_2 concentration exceeding 400 ppmv. The CO_2 activity factor has not been activated in the reference simulation. Its activation increases the global isoprene emission by 2.5 %.

At the regional scale, the annual totals (Fig. 1) are very similar to the totals reported by Sindelarova et al. (2014) for isoprene and Messina et al. (2015) for isoprene and other compounds. Highest emissions occur in South America, Africa, South Asia, Australia and North America. The similarity in the spatial distribution of emissions results from the use of the same emission factor distributions (obtained from global emission factor maps and MEGAN-CLM4 PFT fractions) in the three studies. This result confirms that in the MEGAN model the spatial emission distribution mainly depends on the emission factor and PFT distributions, since the meteorological drivers are different between these studies.

Seasonal variations of the emissions of isoprene, monoterpenes and other compounds are also in line with the results of Messina et al. (2015), despite the use of different LAI distributions. Both results agree on a net maximum of emission in July for all the selected compounds, except isoprene which has a more constant seasonal emission profile with higher emissions in March and July and lower emissions in June. Thus, the use of the LAI distribution calculated with the JSBACH model instead of MODIS derived LAI does not significantly modify neither the spatial distribution nor the seasonal profile of the emissions. Sindelarova et al. (2014) however report a slightly different emission profile in comparison to this study and to Messina et al. (2015), with a shifted isoprene emission maximum around October/November and a minimum in June, and a maximum of monoterpene emissions extended to July/August and beginning of September. The differences in the seasonal emission features are thus mainly due to the differences in the climatic forcing used in the three studies, climate variables (here temperature and radiation) being main drivers of the inter-annual fluctuations of emissions (Guenther et al., 2012).

4.3 Sensitivity simulations

This section presents the sensitivity of emission estimates with the biogenic module in ECHAM-HAMMOZ to a selection of model input parameters and parameterizations related to land and vegetation cover (emission factors, PFT distributions and soil water). We also analyze the effect of nudging climate in different configurations of the biogenic module. The impacts on the emissions are showed only for the most abundant BVOCs. A detailed list of emission estimates for the 32 compounds simulated with the biogenic module is given in Supplementary Material, Sect. S4.

Sensitivity of BVOC emissions to different LAI distributions has not been tested here separately, as the use of JSBACH derived LAI does not lead to significant changes in the emission distributions. LAI impact could be of importance if changing dynamically the vegetation cover in response to land-use and future climate changes. Scaling the LAI by a factor 1.5 in an additional sensitivity simulation leads to an increase of isoprene and monoterpene global annual emissions (averaged over the simulation period 2000-2012) by 18.5 % and 16.5 %, respectively, in comparison to the reference simulation. The effect of LAI change in the biogenic module is larger in comparison to the global annual increases of isoprene and monoterpene emissions for the same sensitivity test with MEGANv2.1 reported in Messina et al. (2015) as 6.6 % and 6 %, respectively. The larger sensitivity of emissions to LAI we obtain here can be explained notably by the formulation of the LAI activity factor, which has a larger increase rate for low LAI, and the slightly lower values of LAI used in the present study in comparison to the reference LAI distribution used in Messina et al. (2015) (not showed).

4.3.1 Impact of PFT-dependent emission factors

The impact of emission factors on the emissions calculated with the biogenic module in ECHAM-HAMMOZ is evaluated in simulation PFT-CLM4. Here, the emission factors from the global maps of 10 compounds (isoprene, α-pinene, β-pinene, 3-carene, limonene, myrcene, t-β-ocimene, sabinene, 232-MBO and nitric oxide) as used in the CTRL simulation are replaced by emission factor distributions derived from the MEGAN2.1-CLM4 PFT fractions (as explained in Sect. 2.3.2). Global and regional relative differences of the annual emissions of the 10 compounds listed above are shown in Fig. 5. Globally, isoprene emissions decrease by 8.5 % in experiment PFT-CLM4, resulting from a decrease of emission mainly in Australia, but also in Africa, Northern America and Russia. However, isoprene emissions increase in South America and South Asia. Sindelarova et al. (2014) report a global decrease of 12.5 % for the same sensitivity experiment, and similar regional distribution of the impacts. The difference between the two studies can be attributed to the difference in the spatial resolution of the simulations, 1.875° x 1.875° here and 0.5° x 0.5° in Sindelarova et al. (2014), that significantly influences the emission estimates in coastal regions and areas with large variations in topography and land cover (Pugh et al., 2013). However, the impact of emission factors on isoprene emissions obtained here and by Sindelarova et al. (2014) is much higher than the 1 % decrease reported in Guenther et al. (2012). Most of the differences obtained here can be explained directly from the differences in the emission factor distributions. The emission factor maps used in the reference simulation are derived from detailed land cover and plant species distributions, as well as above canopy flux measurements, and thus account for species composition variability (Guenther et al., 2012). For the PFT-based emission factor distributions used in the PFT-CLM4 simulation, each PFT is associated to a constant value of emission factor per compound, which is an average of the plant species specific emission factors for the plant species belonging to that particular PFT. For some PFTs, grouping together species with comparable emissions, the differences are small, but for PFTs grouping together high and low emitter plant species, this can lead to significant discrepancies. For example, Broadleaf Deciduous Temperate Trees PFT groups together *Acer* with negligible isoprene emissions and *Quercus* with high isoprene emissions. Switching to this PFT-specific emission factor thus lowers isoprene emission in the regions covered by *Quercus*. The biogenic emission module is highly sensitive to changes in emission factors. The modification of the emission factor distribution mainly affects the spatial distribution of the simulated BVOC emissions, but does not impact the seasonality of the emissions.

As shown in Fig. 6, the increase of isoprene emission in tropical regions in the PFT-CLM4 simulation results directly from the higher constant values of emission factors associated to tropical PFTs. The decrease of isoprene emission in Australia and sub-Saharan Africa is directly linked to the covering of these regions with mainly temperate shrub and grass PFTs in the MEGAN2.1-CLM4 PFT distribution, associated to lower constant emission factors. Moreover, the MEGAN2.1-CLM4 PFT distribution does not reproduce the presence of temperate and tropical species with higher emission factors, especially in the North of Australia. In the Northern part of North America and in Siberia, isoprene emission factors associated to temperate and boreal PFTs, dominant in these regions, are lower than the species-specific emission factors. However, despite the significant lowering of emission factors in Northern regions, isoprene emission are only slightly decreased in comparison to tropical regions. This is mainly due to the lower rate of isoprene emissions in cooler climatic conditions (Guenther et al., 2006).

Monoterpene emissions are strongly impacted by the use of PFT-specific emission factors. At the global scale, α-pinene and myrcene emissions increase by respectively 75 % and 157 %, whereas t-β-ocimene emission decreases by 25 %. Large increases of all monoterpene compounds occur in Australia in the PFT-CLM4 simulation, due to the presence of temperate shrub PFTs, strong monoterpene emitters, in major part of Australia. Similarly to isoprene, α-pinene and myrcene emissions increase strongly in South America (+125 % for α-pinene and +300 % for myrcene) in response to larger spatial coverage of tropical vegetation with high emission factors in the MEGAN2.1-CLM4 PFT distribution. In Northern regions, α-pinene emissions also increase (+82 % in North America) in response to the high values of emission factors associated to needleleaf evergreen temperate and boreal PFTs, mainly covering these regions in the PFT-CLM4 simulation. However, t-β-ocimene emissions decrease in all regions except Australia (for example, -34 % in South America, -39 % in Europe). This is due to the slightly lower emission factor associated to tropical and temperate PFTs for t-β-ocimene.

232-MBO and nitric oxide emissions are also significantly affected by the use of PFT-dependent emission factors. 232-MBO and nitric oxide emissions decrease by 18 % and 38 %. 232-MBO emissions increase strongly in Europe and Russia, but decrease in the rest of the world, whereas nitric oxide emissions decrease in all regions. As shown in Fig. 6, the decrease of 232-MBO emissions in tropical regions is due to very low emission factor values associated to temperate and tropical PFTs (between 0.0002 and 0.04 mg C m^{-2} day^{-1}) in comparison to the emission factor values deduced from global maps (between 0.1 and 0.5 mg C m^{-2} day^{-1}). Much higher values of emission factors associated to needleleaf evergreen temperate and boreal tree PFTs (PFTs 1 and 2 in the MEGAN2.1-CLM4 PFT classification, with emission factors of respectively 14.4 and 1.23 mg C m^{-2} day^{-1}) lead to a strong increase of 232-MBO emissions in northern regions and particularly in Northern Europe and Russia mainly covered by PFTs 1 and 2. However, the PFT-based emissions factors are still lower than the species-specific values obtained from the global maps in North America, explaining the decrease in 232-MBO in several areas.

4.3.2 Impact of PFT distribution

In simulation PFT-JSBACH, the MEGAN2.1-CLM4 PFT distribution is replaced by the extended-JSBACH PFT distribution. As explained in Sect. 2.3.2, the extended-JSBACH 14-PFT classification has been developed to be as similar as possible to the MEGAN2.1-CLM4 15-PFT classification, in order to use the emission factors associated to the MEGAN2.1-CLM4 PFTs for the extended-JSBACH PFTs. Therefore, differences in BVOC emissions between simulations PFT-JSBACH and PFT-CLM4 only results from the differences in the PFT geographical distribution and fractional coverage of the grid-cells. Table 6 lists the global continental areas covered by the 14 PFTs of the MEGAN2.1-CLM4 and extended-JSBACH classifications and Fig. 7 illustrates the distribution of dominant PFTs for both classifications. Tropical and temperate tree PFTs are generally less extended in the JSBACH distribution. The areas covered by Broadleaf Deciduous Temperate and Tropical trees (PFT 2 and 7) are particularly reduced, whereas boreal tree PFTs cover larger areas. The areas covered by shrub PFTs are also lowered, especially for the boreal shrubs (PFT 10) which are replaced by cool/cold C3 grasses or bare soil at high latitudes of the Northern Hemisphere in the JSBACH distribution. Differences also occur in the grass and crop PFT distributions, but only slightly impact BVOC emissions due to the lower emission factors associated to these PFTs.

At the global scale, all BVOC emissions decrease in the PFT-JSBACH experiment in comparison to the PFT-CLM4 experiment mainly in response to the reduction of the spatial extent of tropical PFTs (PFT 1 and 2). The seasonality of emission is not affected by the change in PFT distribution. Isoprene and monoterpene emissions are reduced by about 9 %, methanol and acetone by 17 %, and beta-caryophyllene by 20 % (Fig. 8). The global reduction of isoprene emission due to PFT distribution change we have obtained here is less than the 13 to 24 %, and 30 % impact reported respectively in Guenther et al. (2006) and Pfister et al. (2008). In these two studies, the PFT distributions used to force the MEGAN model were mainly obtained from MODIS satellite observations using different procedures to assign PFT coverage. This caused large differences in PFT distributions and area estimates, and thus in isoprene emissions.

As shown in Fig. 9, the decrease of isoprene, α-pinene (and other monoterpenes) and β-caryophyllene annual emissions occurs mainly in tropical regions, due to the reduction of the spatial extension of tropical PFTs in the extended-JSBACH distribution, particularly in Indonesia and South Asia (see Fig. 10), which are strong emitters of most of compounds. However, the extension of broadleaf deciduous tropical trees (PFT 2) in Central Africa, India and the South of China leads to higher emissions in these regions. In agreement with the results of Guenther et al. (2006) and Pfister et al. (2008), we observe here that isoprene emissions are mostly impacted by the differences in the coverage of broadleaf trees and shrubs, that are the vegetation classes with the highest emission factors. Changes in crop, grass and needleleaf trees distributions have a smaller effect. Moreover, the effect of tropical PFT on the emissions are also reinforced by the year-long warm temperatures and high incoming radiation of tropical regions inducing higher activity factors, and thus higher emission rates. This effect is also illustrated by the relatively low impact of the modification in the boreal PFT distributions on isoprene emission. Indeed, despite the expansion at mid- and high latitudes of the Northern Hemisphere of Broadleaf Deciduous Boreal trees (PFT 8), associated to high isoprene emission potential, isoprene emission are only slightly increased due to the lower values of activity factors for light and temperature in these regions.

232-MBO emissions are significantly decreased in Northern regions in response to the reduction of the fractions of Needleleaf Evergreen Temperate and Boreal trees (PFT 3 and 4). 232-MBO has the same parameterization for light and temperature as isoprene, but it is mainly emitted by boreal and cold tree species and its emission factor for Needleleaf Evergreen Temperate trees (PFT 3) is about 70,000 times its emission factor associated to tropical PFTs. α-pinene and β-caryophyllene emissions also decrease in Northern regions in response to the reduction of PFTs 3 and 4 coverage. These compounds don't have higher emission potentials for cold PFTs in comparison to tropical PFTs, but the different parameterization of the temperature activity factor, including a light-independent function, leads to higher emissions rates and emission sensitivity at high latitudes in comparison to isoprene.

4.3.3 Impact of soil moisture on isoprene emission

The impact of soil moisture on simulated isoprene emission is evaluated in experiment TEST-SM, via the activation of the activity factor γ_{SM} as described by Guenther et al. (2006, 2012). The soil water activity factor is evaluated here using the relative soil water amount (soil water depth relative to the maximum water depth, corresponding here to the root zone (Hagemann and

Stacke, 2015)), and a wilting point set at 35 % of the maximum soil water amount. The detailed parameterization of the γ_{SM} activity factor is given in Supplementary Material, Sect. S1.

The activation of the soil moisture activity factor reduces global isoprene emission by 15.2 %. The soil moisture impact reported here is within the range of previous estimates with the MEGAN model. It is higher than the 1 % and 7 % reductions in isoprene emission reported respectively by Lathière et al. (2010) and Guenther et al. (2006), but less than the 21 % reduction of Müller et al. (2008) and 50% reduction of Sindelarova et al. (2014). All the mentioned studies are based on the same algorithm, thus the differences in the soil moisture effects on isoprene emissions are due only to the use of different soil moisture and wilting point datasets. Wilting point is particularly important since it is the threshold value below which the soil moisture activity factor, and thus the isoprene emissions are set to zero, and has to be consistent with the soil moisture data (Guenther et al., 2012). Nevertheless, the soil moisture impact has to be considered with caution (Müller et al., 2008), because its parameterization is based on measurements from only one study (Pegoraro et al., 2004).

Despite the use of different soil moisture databases, the geographical distribution of the soil moisture activity factor showed in Fig. 11 is very similar to the ones obtained in Müller et al. (2008) and Sindelarova et al. (2014). Arid and semi-arid regions are characterized by γ_{SM} values below 0.5, whereas most of the tropical and temperate regions have γ_{SM} up to 0.9. Our estimates of γ_{SM} are higher than the values reported by Sindelarova et al. (2014) in South Africa, Central Africa and South Asia, but lower than the estimations of Müller et al. (2008) and Sindelarova et al. (2014) in Northern regions, especially in Siberia. Similarly to Müller et al. (2008) and Sindelarova et al. (2014), isoprene emissions mainly decrease in the tropical regions affected by low soil moisture activity factor, i. e. the Southern part of North America, South America, Subsaharan Africa, Central Asia and Australia. The decrease in isoprene emission is particularly marked in the North of Australia, reaching up to 60% of the reference emissions. The soil moisture impact is slightly more pronounced during summer months and dry seasons (not showed), except in Australia where the major part of the annual effect is due to the emission reductions occurring during the Southern Hemisphere summer.

4.3.4 Impact of nudging

Since the soil moisture effect depends primarily on the modeled water cycle, we also tested the impact of running a nudged simulation versus simulations with only prescribed sea surface temperatures and sea ice coverage. Even though nudging in ECHAM6-HAMMOZ does not include nudging to humidity data, the use of surface pressure, temperature, vorticity and divergence from reanalysis has an impact on the water cycle in ECHAM6 (Lohmann and Hoose, 2009; Lohmann and Ferrachat, 2010). The effect of nudging on the biogenic emissions is analyzed in experiments TEST-NUDG and TEST-NUDG+SM. Simulation TEST-NUDG is identical to the reference simulation except that nudging to ERA-Interim data is applied for vorticity, divergence, temperature and surface pressure (Lohmann and Hoose, 2009; Zhang et al., 2014). In simulation TEST-NUDG+SM the nudging and the soil moisture activity factor are activated. Generally, nudging the climate simulation towards global weather reanalysis is applied in order to perform more straightforward comparison between simulation and observation, and also to allow for distinguishing between signal and noise after a shorter simulation time (Zhang et al., 2014). In the experiment TEST-NUDG, nudging has a weak impact on the simulated global biogenic emissions, decreasing the total global emissions by 2.6 %.

Figure 12 gives the annual global relative emission differences for the most emitted and important compounds. Isoprene global annual emissions are reduced by 1.8 % (-7.6 Tg C year^{-1}), which is less than the interannual variability (standard deviation of 9.1 Tg C year^{-1} for the 13 years simulation), monoterpene emissions by 3.6 %, and a maximum decrease of 5.2 % is obtained for β-caryophyllene. The activation of the soil moisture activity factor in the TEST-NUDG+SM simulation leads to similar

5   conclusions. The isoprene global emission is reduced by 17.1 % (relative to the reference simulation), which is about the sum of the soil moisture impact (-15.2 %) and the nudging impact (-1.8 %). By constraining the simulated wind and temperature fields using reanalysis, nudging reduces the BVOC emission variability in agreement with Zhang et al. (2014). As illustrated in Fig. 13 for isoprene and monoterpenes, the interannual and seasonal variations of global emissions in the nudged and reference simulations have mostly similar profiles, but the annual and monthly fluctuations are reduced in the TEST-NUDG simulation

10   in comparison to the reference simulation by 1 Tg C year^{-1} for isoprene and by 0.08 Tg C year^{-1} for monoterpenes in average over the modelled period. The difference between the highest and the lowest global annual emission over the 2000-2012 simulation period is about 8.4 % (5.8 %) of isoprene (monoterpenes) total emission averaged over the simulation period in the reference simulation and 5.5 % (4.9 % for monoterpenes) in the nudged simulation. However, the activation of the soil moisture effect increases the interannual variability of isoprene emissions to 8.8 % in the TEST-NUDG+SM simulation. The

15   temporal profile of the emission is similar to the profile of experiment TEST-NUDG, but shifted to lower annual totals due to the reduction of isoprene emission by the soil moisture effect. The standard deviation of total annual isoprene emissions obtained here ($\pm$ 9.1 Tg C year^{-1}) is lower than the standard deviations of total annual isoprene emissions of $\pm$ 30 Tg C year^{-1} and $\pm$ 20.2 Tg C year^{-1} reported by respectively Müller et al. (2008) (1995-2006 MEGANv2 simulation forced with ECMWF reanalysis) and Sindelarova et al. (2014) (1980-2010 MEGANv2.1 simulation forced with MERRA reanalysis). However, the

20   standard deviation of the reference simulation is closer to the $\pm$ 10.8 Tg C year^{-1} standard deviation obtained by Lathière et al. (2006) for a 1983-1995 simulation using the MEGANv2 model forced with satellite based climate archive. Differences in the isoprene variability can be associated to the differences in the meteorological datasets used in the different studies. The activation of the soil moisture activity factor could partly explain the larger interannual variability in the study of Müller et al. (2008), following the results of experiment TEST-NUDG+SM. The activation of the CO_2 activity factor in Sindelarova et al.

25   (2014) can also lead to larger differences between the global isoprene estimates at the beginning and the end of the temporal series studied.

Nudging has also a weaker impact on the spatial distribution of BVOC emissions in comparison to PFT distributions and emission factors. Effects of nudging are mainly localized in tropical regions (see Fig. 14). Isoprene emissions increase in the South-East of North America, North of South America and the western part of Equatorial Africa, and slightly decrease in South

30   America, India and large parts of Australia. The same distribution of emission differences is observed for α-pinene, but the impacts are more marked in the Northern Hemisphere, with a decrease of emissions in North America, Southern Europe and Russia, and an increase of emissions in Northern Europe. Isoprene and α-pinene emission differences are mainly driven by the differences in surface air temperature and shortwave radiation induced by the nudging of meteorological variables, as showed in Fig. 15. The increase of temperature and radiation in the North of South America, South-East of North America, Western Africa

35   and Northern Europe leads to emission increases, whereas the decrease of temperature in Australia and North America induces

emissions decrease. An exception is observed in India where the emission decrease is not directly linked to the temperature and radiation increase observed there. As discussed in Lohmann and Hoose (2009) and Lohmann and Ferrachat (2010), nudging the ECHAM model only weakly impacts global mean TOA radiation and global temperature. Here, we obtain a global surface air temperature decrease of -0.17°C (most of the regional impacts counterbalancing each others) and a global shortwave

5 surface radiation increase of 4.6 W/m^2. Nudging in ECHAM has a stronger effect on precipitation, generally increasing the convective activity in the tropical regions (Lohmann and Hoose, 2009).The activation of the soil moisture activity factor in TEST-NUDG+SM affects the isoprene emission distribution exactly with the same patterns and intensity as in experiment TEST-SM (not showed). The decrease of isoprene emissions is slightly more marked notably in India and in South America, due to the reduction of soil moisture in these regions in response to the large reduction of precipitation obtained in the nudged

10 experiments (see Fig. 15).

5   Conclusions

A biogenic emission scheme based on the MEGANv2.1 model (Guenther et al., 2012) has been integrated into ECHAM6-HAMMOZ chemistry climate model and linked to parameters of the vegetation model JSBACH, in order to calculate the biogenic emissions of 32 compounds. The model calculates a total emission of 634 Tg C yr^{-1} from terrestrial vegetation

15 over the period 2000-2012 . Isoprene is the main contributor to the average emission total accounting for 66 % (417 Tg C yr^{-1}), followed by several monoterpenes (12 %), methanol (7 %), acetone (3.6 %) and ethene (3.6 %). Tropical regions are identified as the primary source of global BVOCs, contributing to 87 % of isoprene, 79 % of monoterpenes and 73 % of methanol global annual emissions. The standard deviation of total annual isoprene emissions over the studied period is ± 9.1 Tg C year^{-1}, lower than previously reported (Sindelarova et al., 2014; Müller et al., 2008). The biogenic emission estimates

20 in ECHAM6-HAMMOZ are within the range of previous emission budgets obtained with different versions of the MEGAN model. Nevertheless, model estimates of BVOC emissions show a large variation, global isoprene emissions varying within a factor of 1.6, when global monoterpene and methanol emissions vary within a factor of about 3.5. Most of the discrepancies between model emission estimates can be attributed the use of different climatic input data, vegetation related parameters (LAI, PFT distributions), parameterizations and empirical coefficients within the MEGAN model (emission factors, parameteriza-

25 tion of activity factors,...). The variability in BVOC emission estimates using the same model with different configurations highlights the need for a systematic effort to improve the understanding of the key processes and mechanisms responsible for BVOC emissions. Measurements of BVOC emissions in various regions of the Earth and over longer time period, as well as sensitivity tests and model intercomparisons, are therefore required to obtain more accurate emission estimates and refine the model parameterizations.

30   The sensitivity of biogenic emissions to a selection of model input parameters and parameterizations related to vegetation cover and climate have been evaluated in a series of sensitivity simulations. The biogenic model shows a high sensitivity to the changes in PFT distributions and associated emission factors. The use of emission factors derived from PFT distributions instead of gridded maps of species-specific values results in isoprene and α-pinene estimates varying respectively by 8.5 % and

75 % of the reference simulation values, and to the largest changes in the spatial distribution of BVOC emissions in comparison to the other simulation results presented here. These effects are mainly explained by the differences in the PFT spatial coverage and the averaged emission factors associated to each PFT in comparison to the species-specific values. Switching to the PFT distribution derived from the JSBACH vegetation model has a lower impact on BVOC emissions, and causes a decrease of isoprene and monoterpene emissions by about 9 %, that can be mostly attributed to the differences in the distribution of tropical and temperate tree PFTs. Isoprene emissions show the highest sensitivity to soil moisture impact, with a global decrease of isoprene emission by 12.5 % when the soil moisture activity factor is included in the emission parameterization. This effect is within the broad range of previous results of sensitivity studies, varying from 1 % (Lathière et al., 2010) to 50 % (Sindelarova et al., 2014). The large uncertainties concerning the soil moisture impact on isoprene emissions are mainly explained by the use of different soil moisture and wilting point databases. This also highlights the need of a better understanding and more constrained parameterization of the soil moisture impact on isoprene and the introduction of its impact on other compounds in the MEGAN model as suggested by Wu et al. (2015). Nudging ECHAM6 climate towards ERA-Interim reanalysis has a much lower impact on the biogenic emissions in comparison to the effects of PFT distributions and soil moisture. Constraining meteorological variables lowers the interannual variability in comparison to the reference simulation, and most of the regional impacts can be explained by the slight differences obtained in temperature and radiation.

The results of the present study demonstrate the capability of the biogenic model embedded in ECHAM6-HAMMOZ in reasonably representing BVOC emissions at the global and regional scales. This version of the ECHAM6-HAMMOZ model is now suitable for many tropospheric investigations, notably concerning the impact of BVOC emissions on the ozone budget, secondary aerosol formation and atmospheric chemistry. Activating the dynamic vegetation component of the JSBACH model also allows for the study of present-day and future land cover and land-use change impacts on atmospheric chemistry in a comprehensive chemistry climate model framework.

6   Code availability

The code of the biogenic module (Fortran 95) is available upon request from the corresponding author or as part of the ECHAM6-HAMMOZ chemistry climate model through the HAMMOZ distribution web page https://redmine.hammoz.ethz. ch/projects/hammoz.

Author contributions.   A.-J. Henrot implemented the biogenic module into the atmospheric chemistry model and performed the simulations. T. Stanelle and C. Siegenthaler worked on the link between the biogenic module and the vegetation model JSBACH. D. Taraborrelli and S. Schröder helped in model developments. M. G. Schultz supervised the whole work and especially the design of the experiments. A.-J. Henrot prepared the manuscript with contributions from all co-authors.

Competing interests.   The authors declare that they have no conflict of interest.

Acknowledgements. We are grateful to Christian Reick for discussions on model developments and results. We appreciated the useful and constructive comments and corrections of the three anonymous referees. This research is based upon work co-funded by the European Union (BeIPD- Marie Curie COFUND). The ECHAM-HAMMOZ model is developed by a consortium composed of ETH Zurich, Max Planck Institut für Meteorologie, Forschungszentrum Jülich, University of Oxford, the Finnish Meteorological Institute and the Leibniz Institute for

5   Tropospheric Research, and managed by the Center for Climate Systems Modeling (C2SM) at ETH Zurich.

References

Arneth, A., Niinemets, U., Pressley, S., Bäck, J., Hari, P., Karl, T., Noe, S., Prentice, I. C., Serça, D., Hickler, T., Wolf, A., and Smith, B.: Process-based estimates of terrestrial ecosystem isoprene emissions: incorporating the effects of a direct CO_2-isoprene interaction, Atmos. Chem. Phys., 7, 31–53, 2007.

5 Arneth, A., Schurgers, G., Lathière, J., Duhl, T., Beerling, D. J., Hewitt, C. N., Martin, M., and Guenther, A.: Global terrestrial isoprene emission models: sensitivity to variability in climate and vegetation, Atmos. Chem. Phys., 11, 8037–8052, 2011.

Ashworth, K., Boissard, C., Folberth, G., Lathière, J., and Schurgers, G.: Global Modelling of Volatile Organic Compound Emissions, in: Biology, Controls and Models of Tree Volatile Organic Compound Emissions, edited by Niinemets, U. and Monson, R. K., chap. 16, pp. 451–489, Springer, Berlin, 2013.

10 Atkinson, R. and Arey, J.: Gas-phase tropospheric chemistry of biogenic volatile organic compounds: a review, Atmos. Environ., 37, 197–219, 2003.

Brovkin, V., Raddatz, T., Reick, C., Claussen, M., and Gayler, V.: Global biogeophysical interactions between forest and climate, Geophys. Res. Lett., 36, L07 405, 2009.

Brovkin, V., Boysen, L., Raddatz, T., Gayler, V., Loew, A., and Claussen, M.: Evaluation of vegetation cover and land-surface albedo in
15 MPI-ESM CMIP5 simulations, J. Adv. Model. Earth Syst., 5, 48–57, 2013.

Cabrera-Perez, D., Taraborrelli, D., Sander, R., and Pozzer, A.: Global atmospheric budget of simple monocyclic aromatic compounds, Atmos. Chem. Phys., 16, 6931–6947, 2016.

Collins, W. J., Derwent, R. G., Johnson, C. E., and Stevenson, D. S.: The oxidation of organic compounds in the troposphere and their global warming potentials, Climatic Change, 52, 453–479, 2002.

20 Constable, J. V. H., Litvak, M. E., Greenberg, J. P., and Monson, R. K.: Monoterpene emission from coniferous trees in response to elevated CO_2 concentration and climate warming, Global Change Biol., 5, 255–267, 1999.

Crippa, M., Janssens-Maenhout, G., Dentener, F., Guizzardi, D., Sindelarova, K., Muntean, M., Dingenen, R. V., and Granier, C.: Forty years of improvements in European air quality: regional policy-industry interactions with global impacts, Atmos. Chem. Phys., 16, 3825–3841, 2016.

25 Dee, D. P., Uppala, S. M., Simmons, A. J., Berrisford, P., Poli, P., Kobayashi, S., Andrae, U., Balmaseda, M. A., Balsamo, G., Bauer, P., Bechtold, P., Beljaars, A. C. M., van de Berg, L., Bidlot, J., Bormann, N., Delsol, C., Dragani, R., Fuentes, M., Geer, A. J., Haimberger, L., Healy, S. B., Hersbach, H., Holm, E. V., Isaksen, L., Kallberg, P., Khöler, M., Matricardi, M., McNally, A. P., Monge-Sanz, B. M., Morcrette, J.-J., Park, B.-K., Peubey, C., P. de Rosnay and, C. T., Thepaut, J.-N., and Vitart, F.: The ERA-Interim reanalysis: configuration and performance of the data assimilation system, Q. J. R. Meteorol. Soc. A, 137, 553–597, 2011.

30 Emmons, L. K., Walters, S., Hess, P. G., Lamarque, J.-F., Pfister, G. G., Fillmore, D., Granier, C., Guenther, A., Kinnison, D., Laepple, T., Orlando, J., Tie, X., Tyndall, G., Wiedinmyer, C., Baughcum, S. L., and Kloster, S.: Description and evaluation of the Model for Ozone and Related chemical Tracers, version 4 (MOZART-4), Geosci. Model Dev., 3, 43–67, 2010.

Fischer, E. V., Jacob, D. J., Millet, D. B., Yantosca, R. M., and Mao, J.: The role of the ocean in the global atmospheric budget of acetone, Geophys. Res. Lett., 39, L01 807, 2012.

35 Giorgetta, M. A., Jungclaus, J., Reick, C. H., Legutke, S., Bader, J., Böttinger, M., Brovkin, V., Crueger, T., Esch, M., Fieg, K., Glushak, K., Gayler, V., Haak, H., Hollweg, H.-D., Ilyina, T., Kinne, S., Kornblueh, L., Matei, D., Mauritsen, T., Mikolajewicz, U., Mueller, W., Notz, D., Pithan, F., Raddatz, T., Rast, S., Redler, R., Roeckner, E., Schmidt, H., Schnur, R., Segschneider, J., Six, K. D., Stockhause,

M., Timmreck, C., Wegner, J., Widmann, H., Wieners, K.-H., Claussen, M., Marotzke, J., and Stevens, B.: Climate and carbon cycle changes from 1850 to 2100 in MPI-ESM simulations for the Coupled Model Intercomparison Project phase 5, J. Adv. Model. Earth Syst., 5, 572–597, 2012.

Granier, C., Pétron, G., Müller, J.-F., and Brasseur, G.: The impact of natural and anthropogenic hydrocarbons on the tropospheric budget of carbon monoxide, Atmos. Environ., 34, 5255–5270, 2000.

Guenther, A. B., Zimmerman, P. R., Harley, P. C., Monson, R. K., and Fall, R.: Isoprene and monoterpene emission rate variability: Model evaluations and sensitivity analyses, J. Geophys. Res., 98, 12609–12617, 1993.

Guenther, A. B., Hewitt, C. N., Erickson, D., Fall, R., Geron, C., Graedel, T., Harley, P., Klinger, L., Lerdau, M., Mckay, W. A., Pierce, T., Scholes, B., Steinbrecher, R., Tallamraju, R., Taylor, J., and Zimmerman, P.: A global model of natural volatile organic compound emissions, J. Geophys. Res., 100, 8873–8892, 1995.

Guenther, A. B., Karl, T., Harley, P., Wiedinmyer, C., Palmer, P. I., and Geron, C.: Estimates of global terrestrial isoprene emissions using MEGAN (Model of Emissions of Gases and Aerosols from Nature), Atmos. Chem. Phys., 6, 3181–3210, 2006.

Guenther, A. B., Jiang, X., Heald, C. L., Sakulyanontvittaya, T., Duhl, T., Emmons, L. K., and Wang, X.: The Model of Emissions of Gases and Aerosols from Nature version 2.1 (MEGAN2.1): an extended and updated framework for modeling biogenic emissions, Geosci. Model Dev., 5, 1471–1492, 2012.

Hagemann, S. and Stacke, T.: Impact of the soil hydrology scheme on simulated soil moisture memory, Clim. Dyn., 44, 1731, 2015.

Hallquist, M., Wenger, J. C., Baltensperger, U., Rudich, Y., Simpson, D., Claeys, M., Dommen, J., Donahue, N. M., George, C., Goldstein, A. H., Hamilton, J. F., Herrmann, H., Hoffmann, T., Linuma, Y., Jang, M., Jenkin, M. E., Jimenez, J. L., Kiendler-Scharr, A., Maenhaut, W., McFiggans, G., Mentel, T. F., Monod, A., Prévôt, A. S. H., Seinfeld, J. H., Surratt, J. D., Szmigielski, R., and Wildt, J.: The formation, properties and impact of secondary organic aerosol: current and emerging issues, Atmos. Chem. Phys., 9, 5155–5236, 2009.

Heald, C. L., Henze, D. K., Horowitz, L. W., Feddema, J., Lamarque, J.-F., Guenther, A., Hess, P. G., Vitt, F., Seinfeld, J. H., Goldstein, A. H., and Fung, I.: Predicted change in global secondary organic aerosol concentrations in response to future climate, emissions, and land use change, J. Geophys. Res., 113, D05211, 2008.

Heald, C. L., Wilkinson, M. J., Monson, R. K., Alo, C. A., Wang, G., and Guenther, A.: Response of isoprene emission to ambient CO_2 changes and implications for global budgets, Global Change Biol., 15, 1127–1140, 2009.

Jacob, D. J., Field, B. D., Jin, E. M., Bey, I., Li, Q., Logan, J. A., and Yantosca, R. M.: Atmospheric budget of acetone, J. Geophys. Res., 107, D104100, 2002.

Jacob, D. J., Field, B. D., Li, Q., Blake, D. R., de Gouw, J., Warneke, C., Hansel, A., Wisthaler, A., Singh, H. B., and Guenther, A.: Global budget of methanol: Constraints from atmospheric observations, J. Geophys. Res., 110, D08303, 2005.

Lamarque, J.-F., Emmons, L. K., Hess, P. G., Kinnison, D. E., Tilmes, S., Vitt, F., Heald, C. L., Holland, E. A., Lauritzen, P. H., Neu, J., Orlando, J. J., Rasch, P. J., and Tyndall, G. K.: CAM-chem: description and evaluation of interactive atmospheric chemistry in the Community Earth System Model, Geosci. Model Dev., 5, 369–411, 2012.

Lathière, J., Hauglustaine, D. A., Friend, A. D., Noblet-Ducoudré, N. D., Viovy, N., and Folberth, G. A.: Impact of climate variability and land use changes on global biogenic volatile organic compound emissions, Atmos. Chem. Phys., 6, 2129–2146, 2006.

Lathière, J., Hewitt, C. N., and Beerling, D. J.: Sensitivity of isoprene emissions from the terrestrial biosphere to 20th century changes in atmospheric CO_2 concentration, climate, and land use, Global Biogeochem. Cycles, 24, GB1004, 2010.

Lawrence, D. M. and Chase, T. N.: Representing a new MODIS consistent land surface in the Community Land Model (CLM 3.0), J. Geophys. Res.-Biogeo., 112, G01023, 2007.

Lawrence, D. M., Oleson, K. W., Flanner, M. G., Thornton, P. E., Swenson, S. C., Lawrence, P. J., Zeng, X., Yang, Z.-L., Levis, S., Sakaguchi, K., Bonan, G. B., and Slater, A. G.: Parameterization improvements and functional and structural advances in version 4 of the Community Land Model, J. Adv. Model. Earth Syst., 3, M03 001, 2011.

Levis, S., Wiedinmyer, C., Bonan, G. B., and Guenther, A.: Simulating biogenic volatile organic compound emissions in the Community Climate System Model, J. Geophys. Res., 108, D214 659, 2003.

Levis, S., Bonan, G. B., Vertenstein, M., and Oleson, K. W.: The Community Land Model's Dynamic Global Vegetation Model (CLM-DGVM): Technical Description and User's Guide, Tech. Rep. NCAR/TN-459+IA, NCAR, Boulder, Colorado, USA, 2004.

Li, Z. and Sharkey, T. D.: Molecular and pathway controls on biogenic volatile organic compound emissions, in: Biology, Controls and Models of Tree Volatile Organic Compound Emissions, edited by Niinemets, U. and Monson, R. K., chap. 5, pp. 119–151, Springer, Berlin, 2013.

Lohmann, U. and Ferrachat, S.: Impact of parametric uncertainties on the present-day climate and on the anthropogenic aerosol effect, Atmos. Chem. Phys., 10, 11 373–11 383, 2010.

Lohmann, U. and Hoose, C.: Sensitivity studies of different aerosol indirect effects in mixed-phase clouds, Atmos. Chem. Phys., 9, 8917–8934, 2009.

Martin, M., Stirling, C., Humphries, S., and Long, S.: A process-based model to predict the effects of climatic change on leaf isoprene emission rates, Ecol. Model., 131, 161–174, 2000.

Messina, P., Lathière, J., Sindelarova, K., Vuichard, N., Granier, C., Ghattas, J., Cozic, A., and Hauglustaine, D. A.: Global biogenic volatile organic compound emissions in the ORCHIDEE and MEGAN models and sensitivity to key parameters, Atmos. Chem. Phys. Discuss., 15, 33 967–34 033, 2015.

Millet, D. B., Jacob, D. J., Custer, T. G., de Gouw, J. A., Goldstein, A. H., Karl, T., Singh, H. B., Sive, B. C., Talbot, R. W., Warneke, C., and Williams, J.: New constraints on terrestrial and oceanic sources of atmospheric methanol, Atmos. Chem. Phys. Discuss., 8, 6887–6905, 2008.

Millet, D. B., Guenther, A., Siegel, D. A., Nelson, N. B., Singh, H. B., de Gouw, J. A., Warneke, C., Williams, J., Eerdekens, G., Sinha, V., Karl, T., Flocke, F., Apel, E., Riemer, D. D., Palmer, P. I., and Barkley, M.: Global atmospheric budget of acetaldehyde: 3-D model analysis and constraints from in-situ and satellite observations, Atmos. Chem. Phys. Discuss., 10, 3405–3425, 2010.

Misztal, P. K., Hewitt, C. N., Wildt, J., Blande, J. D., Eller, A. S. D., Fares, S., Gentner, D. R., Gilman, J. B., Graus, M., Greenberg, J., Guenther, A. B., Hansel, A., Harley, P., Huang, M., Jardine, K., Karl, T., Kaser, L., Keutsch, F. N., Kiendler-Scharr, A., Kleist, E., Lerner, B. M., Li, T., Mak, J., Nölscher, A. C., Schnitzhofer, R., Sinha, V., Thornton, B., Warneke, C., Wegener, F., Werner, C., Williams, J., Worton, D., Yassaa, N., and Goldstein, A. H.: Atmospheric benzenoid emissions from plants rival those from fossil fuels, Scientific Reports, 5, 12 064, 2015.

Müller, J.-F., Stavrakou, T., Wallens, S., Smedt, I. D., Roozendael, M. V., Potosnak, M. J., Rinne, J., Munger, B., Goldstein, A., and Guenther, A. B.: Global isoprene emissions estimated using MEGAN, ECMWF analyses and a detailed canopy environment model, Atmos. Chem. Phys., 8, 1329–1341, 2008.

Niinemets, U., Tenhunen, J. D., Harley, P. C., and Steinbrecher, R.: A model of isoprene emission based on energetic requirements for isoprene synthesis and leaf photosynthetic properties for Liquidambar and Quercus, Plant Cell Environ., 22, 1319–1335, 1999.

O'Donnell, D., Tsigaridis, K., and Feichter, J.: Estimating the direct and indirect effects of secondary organic aerosols using ECHAM5-HAM, atmos. Chem. Phys., 11, 8635–8659, 2011.

Oleson, K. W., Lawrence, D. M., Bonan, G. B., Flanner, M. G., Kluzek, E., Lawrence, P. J., Levis, S., Swenson, S. C., Thornton, P. E., Dai, A., Decker, M., Dickinson, R., Feddema, J., Heald, C. L., Hoffman, F., Lamarque, J.-F., Mahowald, N., Niu, G.-Y., Qian, T., Randerson, J., Running, S., Sakaguchi, K., Slater, A., Stöckli, R., Wang, A., Yang, Z.-L., Zeng, X., and Zeng, X.: Technical description of version 4.0 of the Community Land Model (CLM), Tech. Rep. TN-478+STR, NCAR, Boulder, Colorado, USA, 2010.

5   Pacifico, F., Harrison, S. P., Jones, C., and Sitch, S.: Isoprene emission and climate, Atmos. Environ., 43, 6121–6135, 2009.

Pegoraro, E., Rey, A., Greenberg, J., Harley, P., Grace, J., Malhi, Y., and Guenther, A.: Effect of drought on isoprene emission rates from leaves of Quercus virginiana Mill, Atmos. Environ., 38, 6149–6156, 2004.

Pfister, G. G., Emmons, L. K., Hess, P. G., Lamarque, J.-F., Orlando, J. J., Walters, S., Guenther, A., Palmer, P. I., and Lawrence, P. J.: Contribution of isoprene to chemical budgets: A model tracer study with the NCAR CTM MOZART-4, J. Geophys. Res., 113, D05 308, 2008.

Pierce, T. E. and Waldruff, P. S.: Pc-Beis - a Personal-Computer Version of the Biogenic Emissions Inventory System, J. Air Waste Manage. Assoc., 41, 937–941, 1991.

Pongratz, J., Reick, C., Raddatz, T., and Claussen, M.: A Global Land Cover Reconstruction AD 800 to 1992 - Technical Description, Tech. Rep. 51, Max-Planck-Institut für Meteorologie, Hamburg, 2008.

15   Pongratz, J., Reick, C., Raddatz, T., and Claussen, M.: Effects of anthropogenic land cover change on the carbon cycle of the last millennium, Global Biogeochem. Cycles, 23, GB4001, 2009.

Pugh, T. A. M., Ashworth, K., Wild, O., and Hewitt, C. N.: Effects of the spatial resolution of climate data on estimates of biogenic isoprene emissions, Atmos. Environ., 70, 1–6, 2013.

Raddatz, T. C., Reick, C., Knorr, W., and Kattge, J.: Will the tropical land biosphere dominate the climate-carbon cycle feedback during the

20   twenty-first century?, Climate Dyn., 29, 565–574, 2007.

Ramankutty, N. and Foley, J. A.: Estimating historical changes in global land cover: croplands from 1700 to 1992, Global Biogeochem. Cycles, 13, 997–1027, 1999.

Ramankutty, N., Evan, A., Monfreda, C., and Foley, J. A.: Farming the planet: 1. Geographic distribution of global agricultural lands in the year 2000, Global Biogeochem. Cycles, 22, GB1003, 2008.

25   Reick, C. H., Raddatz, T., Brovkin, V., and Gayler, V.: Representation of natural and anthropogenic land cover change in MPI-ESM, J. Adv. Model. Earth Syst., 5, 459–482, 2013.

Rinne, J.: Interactive comment on "Global biogenic volatile organic compound emissions in the ORCHIDEE and MEGAN models and sensitivity to key parameters" by P. Messina et al., Atmos. Chem. Phys. Discuss., 15, C11 977–C11 979, 2016.

Roeckner, E., Bäuml, G., Bonaventura, L., Brokopf, R., Esch, M., Giorgetta, M., Hagemann, S., Kirchner, I., Kornblueh, L., Manzini, E.,

30   Rhodin, A., Schlese, U., Schulzweida, U., and Tompkins, A.: The atmospheric general circulation model ECHAM5. Part I : Model description, Tech. Rep. 349, Max-Planck-Institut für Meteorologie, Hamburg, 2003.

Rosenstiel, T. N., Potosnak, M. J., Griffin, K. L., Fall, R., and Monson, R. K.: Increased CO_2 uncouples growth from isoprene emission in an agriforest ecosystem, Nature, 421, 256–259, 2003.

Sindelarova, K., Granier, C., Bouarar, I., Guenther, A., Tilmes, S., Stavrakou, T., Müller, J.-F., Kuhn, U., Stefani, P., and Knorr, W.: Global

35   data set of biogenic VOC emissions calculated by the MEGAN model over the last 30 years, Atmos. Chem. Phys., 14, 9317–9341, 2014.

Sitch, S., Smith, B., Prentice, I. C., Arneth, A., Bondeau, A., Cramer, W., Kaplan, J. O., Levis, S., Lucht, W., Sykes, M. T., Thonicke, K., and Venevsky, S.: Evaluation of ecosystem dynamics, plant geography and terrestrial carbon cycling in the LPJ dynamic global vegetation model, Global Change Biol., 9, 161–185, 2003.

Stavrakou, T., Müller, J.-F., De Smedt, I., Van Roozendael, M., van der Werf, G. R., Giglio, L., and Guenther, A.: Global emissions of non-methane hydrocarbons deduced from SCIAMACHY formaldehyde columns through 2003-2006, Atmos. Chem. Phys., 9, 3663–3679, 2009.

Stavrakou, T., Guenther, A., Razavi, A., Clarisse, L., Clerbaux, C., Coheur, P.-F., Hurtmans, D., Karagulian3, F., Mazière, M. D., Vigouroux, C., Amelynck, C., Schoon, N., Laffineur, Q., Heinesch, B., Aubinet, M., Rinsland, C., and Müller, J.-F.: First space-based derivation of the global atmospheric methanol emission fluxes, Atmos. Chem. Phys., 11, 4873–4898, 2011.

Stevens, B., Giorgetta, M., Esch, M., Mauritsen, T., Crueger, T., Rast, S., Salzmann, M., Schmidt, H., Bader, J., Block, K., Brokopf, R., Fast, I., Kinne, S., Kornblueh, L., Lohmann, U., Pincus, R., Reichler, T., and Roeckner, E.: Atmospheric component of the MPI-M Earth System Model: ECHAM6, J. Adv. Model. Earth Syst., 5, 146–172, 2013.

Stier, P., Feichter, J., Kinne, S., Kloster, S., Vignati, E., Wilson, J., Ganzeveld, L., Tegen, I., Werner, M., Balkanski, Y., Schulz, M., Boucher, O., Minikin, A., and Petzold, A.: The aerosol climate model ECHAM5-HAM, Atmos. Chem. Phys., 5, 1125–1156, 2005.

Tao, Z. and Jain, A. K.: Modeling of global biogenic emissions for key indirect greenhouse gases and their response to atmospheric CO_2 increases and changes in land cover and climate, J. Geophys. Res., 110, D21 309, 2005.

Taraborrelli, D., Lawrence, M., Crowley, J., Dillon, T., Gromov, S., Gross, C., Vereecken, L., and Lelieveld, J.: Hydroxyl radical buffered by isoprene oxidation over tropical forests, Nat. Geosci., 5, 190–193, 2012.

Thomson, A. M., Calvin, K. V., Smith, S. J., Kyle, G. P., Volke, A., Patel, P., Delgado-Arias, S., Bond-Lamberty, B., Wise, M. A., Clarke, L. E., and Edmonds, J. A.: RCP4.5: A pathway for stabilization of radiative forcing by 2100, Climatic Change, 109, 77–94, 2011.

Tilmes, S., Lamarque, J.-F., Emmons, L. K., Kinnison, D. E., Ma, P.-L., Liu, X., Ghan, S., Bardeen, C., Arnold, S., Deeter, M., Vitt, F., Ryerson, T., Elkins, J. W., Moore, F., Spackman, J. R., and Martin, M. V.: Description and evaluation of tropospheric chemistry and aerosols in the Community Earth System Model (CESM1.2), Geosci. Model Dev., 8, 1395–1426, 2015.

van Donkelaar, A., Martin, R. V., Park, R. J., Heald, C. L., Fu, T.-M., Liao, H., and Guenther, A.: Model evidence for a significant source of secondary organic aerosol from isoprene, Atmos. Environ., 41, 1267–1274, 2007.

Velikova, V., Tsonev, T., Pinelli, P., Alessio, G. A., and Loreto, F.: Localized ozone fumigation system for studying ozone effects on photosynthesis, respiration, electron transport rate and isoprene emission in field-grown Mediterranean oak species, Tree Physiol., 25, 1523–1532, 2005.

Wu, C., Pullinen, I., Andres, S., Carriero, G., Fares, S., Goldbach, H., Hacker, L., Kasal, T., Kiendler-Scharr, A., Kleist, E., Paoletti, E., Wahner, A., Wildt, J., and Mentel, T. F.: Impacts of soil moisture on de novo monoterpene emissions from European beech, Holm oak, Scots pine, and Norway spruce, Biogeosciences, 12, 177–191, 2015.

Zhang, K., O'Donnell, D., Kazil, J., Stier, P., Kinne, S., Lohmann, U., Ferrachat, S., Croft, B., Quaas, J., Wan, H., Rast, S., and Feichter, J.: The global aerosol-climate model ECHAM-HAM, version 2: sensitivity to improvements in process representations, Atmos. Chem. Phys., 12, 8911–8949, 2012.

Zhang, K., Wan, H., Liu, X., Ghan, S. J., Kooperman, G. J., Ma, P.-L., Rasch, P. J., Neubauer, D., and Lohmann, U.: Technical Note: On the use of nudging for aerosol-climate model intercomparison studies, Atmos. Chem. Phys., 14, 8631–8645, 2014.

Table 1. Biogenic compound classes and individual compounds included in the biogenic emission module.

Compound Classes	Compound Names
isoprene	isoprene
myrcene	myrcene
sabinene	sabinene
limonene	limonene
3-carene	3-carene
t-β-ocimene	t-β-ocimene
α-pinene	α-pinene
β-pinene	β-pinene
β-caryophyllene	β-caryophyllene
232-MBO	2-methyl-3-buten-2-ol
methanol	methanol
acetone	acetone
carbon monoxide	carbon monoxide
nitric oxide	nitric oxide
bidirectional VOCs	ethanol
	acetaldehyde
	formaldehyde
	acetic acid
	formic acid
stress VOCs	ethene
	hydrogen cyanide
	toluene
other VOCs	methyl bromide
	methyl chloride
	methyl ioide
	dimethyl sulfide
	methane
	ethane
	propane
	butene
	propene
	benzaldehyde

Table 2. Original (11-PFT) and extended (14 PFT) JSBACH PFT classifications for use in the biogenic emission module. The numbers of the corresponding 15 PFTs of the MEGAN2.1-CLM4 classification, as listed in Guenther et al. (2012), are given in italic in parentheses.

JSBACH 11 PFTs	JSBACH extended 14 PFTs (and *corresponding MEGAN2.1-CLM4 PFT number*)	
(1) Tropical Evergreen Trees	(1) Broadleaf Evergreen Tropical Trees *(4)*	
(2) Tropical Deciduous Trees	(2) Broadleaf Deciduous Tropical Trees *(6)*	
(3) Extra Tropical Evergreen Trees {	(3) Needleleaf Evergreen Temperate Trees	*(1)*
	(4) Needleleaf Evergreen Boreal Trees	*(2)*
	(5) Broadleaf Evegreen Temperate Trees	*(5)*
(4) Extra Tropical Deciduous Trees {	(6) Needleleaf Deciduous Boreal Trees	*(3)*
	(7) Broadleaf Deciduous Temperate Trees	*(7)*
	(8) Broadleaf Deciduous Boreal Trees	*(8)*
(5) Raingreen Shrubs	(9) Broadleaf Deciduous Temperate Shrubs *(10)*	
(6) Deciduous Shrubs	(10) Broadleaf Deciduous Boreal Shrubs *(11)*	
(7) C3 Grasses {	(11) Cold/arctic C3 Grasses	*(12)*
	(12) Cool C3 Grasses	*(13)*
(9) C3 Pastures	(12) Cool C3 Grasses *(13)*	
(8) C4 Grasses	(13) Warm C4 Grasses *(14)*	
(10) C4 Pasture	(13) Warm C4 Grasses *(14)*	
(11) C3 and C4 Crops	(14) Crops *(15)*	

Table 3. List of simulations performed.

Experiment	Description
CTRL	reference simulation
PFT-CLM4	use of MEGAN2.1-CLM4 PFT-specific emission factors
PFT-JSBACH	use of JSBACH PFT-specific emission factors
TEST-SM	impact of soil moisture on isoprene (γ_{SM})
TEST-NUDG	impact of climate nudging
TEST-NUDG+SM	impact of climate nudging and soil moisture on isoprene

Table 4. Global annual emission totals averaged over the 12 years (2000-2012) of the reference simulation for the 32 compounds and relative contributions to the global annual emission total. Averaged values are given with the standard deviation σ.

Compound Names	Global annual emission (Tg (species) yr^{-1})	Global annual emission (Tg C yr^{-1})	Relative contribution (%)
isoprene	473±10.2	417±9.1	65.8
methanol	117.1±1.6	43.9±0.6	6.9
α-pinene	29.6±0.5	26.1±0.4	4.1
acetone	36.9±0.5	22.9±0.3	3.6
ethene	26.8±0.4	22.9±0.4	3.6
β-pinene	17.9±0.3	15.8±0.2	2.5
t-β-ocimene	15.9±0.3	14±0.2	2.2
propene	14.8±0.2	12.7±0.2	2.0
ethanol	16.8±0.3	8.8±0.2	1.4
acetaldehyde	16.8±0.3	9.2±0.2	1.4
limonene	9.5±0.1	8.4±0.1	1.3
butene	7.4±0.09	6.3±0.08	1.0
3-carene	6.8±0.1	6±0.1	1.0
sabinene	6.4±0.1	5.7±0.1	0.9
β-caryophyllene	4.8±0.1	4.3±0.1	0.7
myrcene	2.6±0.04	2.3±0.04	0.4
232-MBO	2.4±0.1	2±0.1	0.3
formaldehyde	4.2±0.07	1.7±0.03	0.3
acetic acid	3.1±0.06	1.3±0.02	0.2
toluene	1.4±0.02	1.3±0.02	0.2
formic acid	3.1±0.06	0.8±0.02	0.1
hydrogen cyanide	0.7±0.01	0.3±0.005	0.05
ethane	0.3±0.004	0.3±0.003	0.04
methane	0.15±0.002	0.12±0.001	0.02
methyl chloride	0.3±0.004	0.07±0.0009	0.01
dimethyl sulfide	0.09±0.001	0.04±0.0005	0.006
propane	0.03±0.0004	0.03±0.0003	0.004
benzaldehyde	0.03±0.0004	0.02±0.0003	0.004
methyl bromide	0.06±0.0008	0.01±0.0001	0.001
methyl ioide	0.03±0.0004	0.003±0.0001	0.0004
carbon monoxide	95.8±1.5	41.1±0.6	-
nitric oxide	5.9±0.07	-	-
Total		634.1±12.5	

Table 5. Comparison of several BVOC global total emissions (Tg C year^{-1}) to previous published global totals with different versions of the MEGAN model.

Ref.	Isoprene	Monoterpenes	Methanol	Acetone	Ethene	β-caryophyllene	Acetaldehyde	Formaldehyde	Acetic Acid	Formic Acid	232-MBO	CO
(-)	417	78.3	43.9	22.9	22.9	4.3	9.2	1.7	1.3	0.8	2	41.1
(a)	427.6	74.4	40.9	20.5			8.7	1.6	1.2	0.8	1	
(b)	464.6	91.3	37.8	24.6			8.6	1.9	1.1	0.7	1.3	
(c)	523.7	83.7	48.7	23	15.5		10.4	1.8	1.4	0.9	1.4	38.6
(d)	471.6	124	37.3	24.8	23	6.5	11.4	2	1.5	1	1.9	35
(e)				19.8								
(f)	378											
(g)	393.2	78.5										
(h)			39.3									
(i)	414	80										
(j)	413											
(k)							12.5					
(l)	523											
(m)	469.9											
(n)	361.4											
(o)			30									
(p)	529											
(q)	460	117	106	42			15	10	0.3	1.5		
(r)	601	103										
(s)			48									
(t)	507	33										
(u)				21.7								
(v)	503	127										

(-) This study; (a) MEGANv2.1 off-line, 2000-2009 (Messina et al., 2015); (b) MEGANv2.1 in ORCHIDEE, 2000-2009 (Messina et al., 2015); (c) MEGANv2.1 off-line, 1980-2010 (Sindelarova et al., 2014); (d) MEGANv2.1 in CLM, 2000 (Guenther et al., 2012); (e) MEGANv2 in GEOS-Chem , 2006 (Fischer et al., 2012); (f) MEGANv2 off-line, 1981-2002 (Arneth et al., 2011); (g) MEGANv2 in ECHAM5-HAM, 2000 (O'Donnell et al., 2011); (h) MEGANv2.1 with MOHYCAN canopy (Stavrakou et al., 2011); (i) MEGANv2 in MOZART4, 2000-2007 (Emmons et al., 2010); (j) MEGAN in SDGVM (Lathière et al., 2010); (k) MEGANv2.1 in GEOS-Chem, 2004 (Millet et al., 2010); (l) MEGANv2 in CCSM3, 2000 (Heald et al., 2009); (m) MEGANv2 in MOZART4, 2005 (Pfister et al., 2008); (n) MEGANv2 with MOHYCAN canopy, 1995-2006 (Müller et al., 2008); (o) MEGANv2 in GEOS-Chem, 2004 (Millet et al., 2008); (p) MEGANv2 off-line, 2003 (Guenther et al., 2006); (q) MEGAN in ORCHIDEE, 1983-1995 (Lathière et al., 2006); (r) MEGAN in ISAM, 1981-2000 (Tao and Jain, 2005); (s) MEGAN in GEOS-Chem, 2001 (Jacob et al., 2005); (t) MEGAN in CLM, 1990 (Levis et al., 2003); (u) MEGAN in GEOS-Chem, 1993-1994 (Jacob et al., 2002); (v) MEGAN, 1990 (Guenther et al., 1995)

Table 6. Continental surface areas covered by the MEGAN2.1-CLM4 PFTs and the extended-JSBACH PFTs (10^{12} m^2).

PFT number and name	MEGAN2.1-CLM4 PFT surface	extended-JSBACH PFT surface
0 Bare soil	55.4	85.8
1 Broadleaf Evergreen Tropical Trees	14.1	11.75
2 Broadleaf Deciduous Tropical Trees	8.19	2.98
3 Needleleaf Evergreen Temperate Trees	4.77	1.52
4 Needleleaf Evergreen Boreal Trees	10.68	8.22
5 Broadleaf Evergreen Temperate Trees	2.18	1.25
6 Needleleaf Deciduous Boreal Trees	1.49	2.24
7 Broadleaf Deciduous Temperate Trees	5.32	1.81
8 Broadleaf Deciduous Boreal Trees	1.98	3.19
9 Broadleaf Deciduous Temperate Shrubs	6.32	3.62
10 Broadleaf Deciduous Boreal Shrubs	8.97	1.15
11 Cold/arctic C3 Grasses	4.66	4.32
12 Cool C3 Grasses	13.56	11.54
13 Warm C4 Grasses	12.46	16.25
14 Crops	13.96	10.45
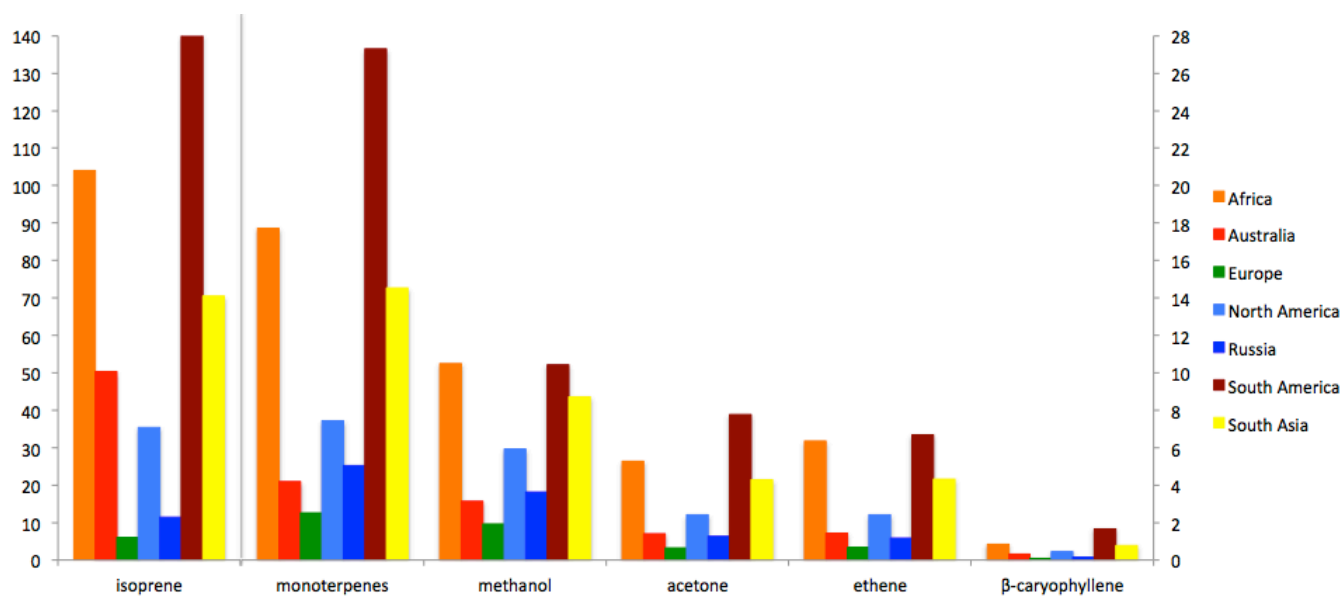
Figure 1. Regional annual emissions (Tg C yr^{-1}) for isoprene, the sum of monoterpenes, methanol, acetone, ethene and β-caryophyllene averaged over the 12 years (2000-2012) of the reference simulation. y-axes scales are separated for isoprene and the other compounds. The geographical regions considered here are Africa (-35° to 37° Nord and -20° to 65° East), Australia (-50° to -10° Nord and 110° to 179° East), Europe (36° to 75° Nord and -15° to 50° East), North America (13° to 75° Nord and -170° to -40° East), Russia (37° to 75° Nord and 50° to 179° East), South America (-60° to 5° Nord and -90° to -36° East) and South Asia (-10° to 37° Nord and 110° to 179° East).
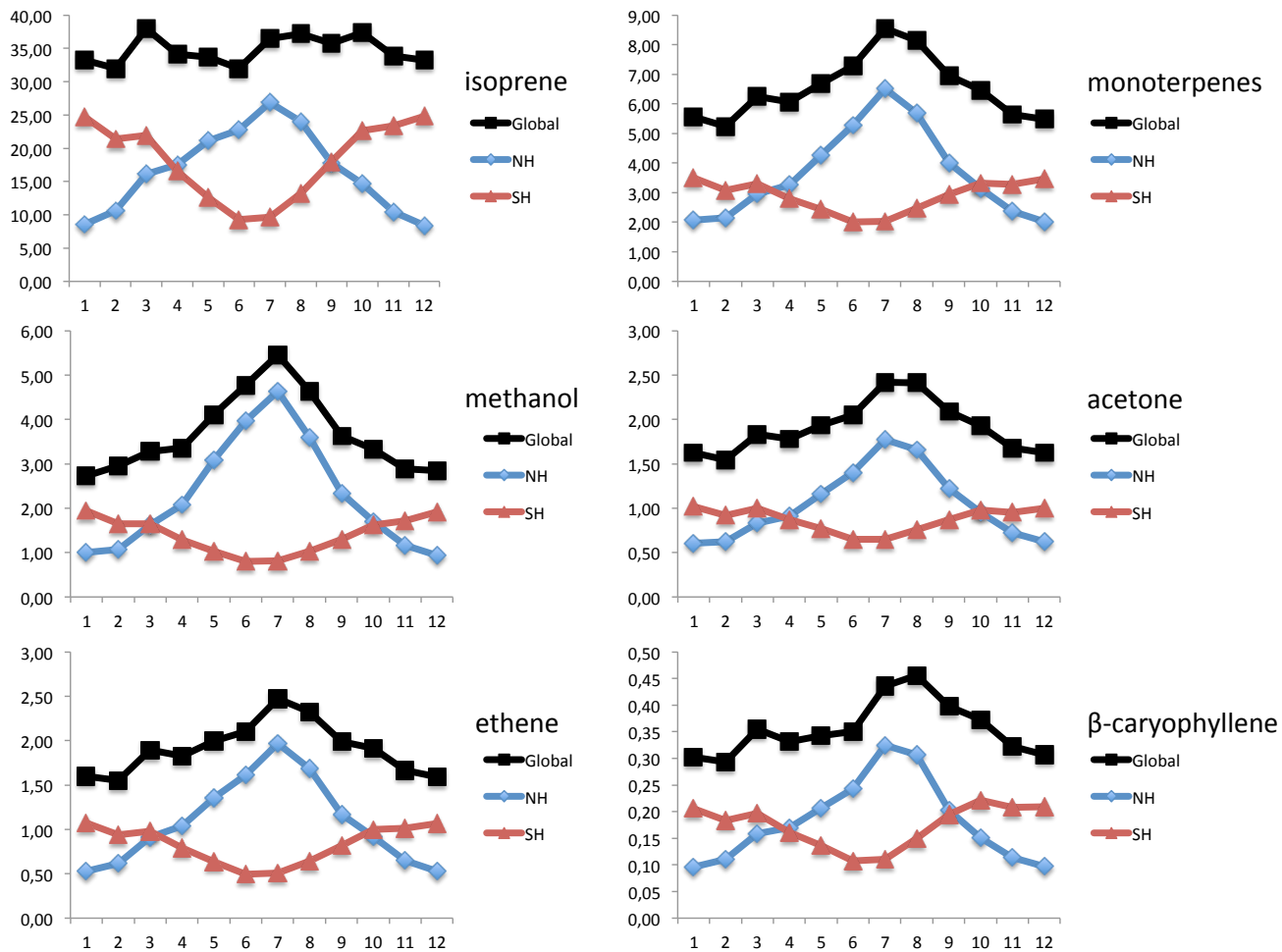
Figure 2. Global, Northern and Southern Hemispheres monthly emissions (Tg C month^{-1}) for isoprene, the sum of monoterpenes, methanol, acetone, ethene and β-caryophyllene averaged over the 12 years (2000-2012) of the reference simulation.
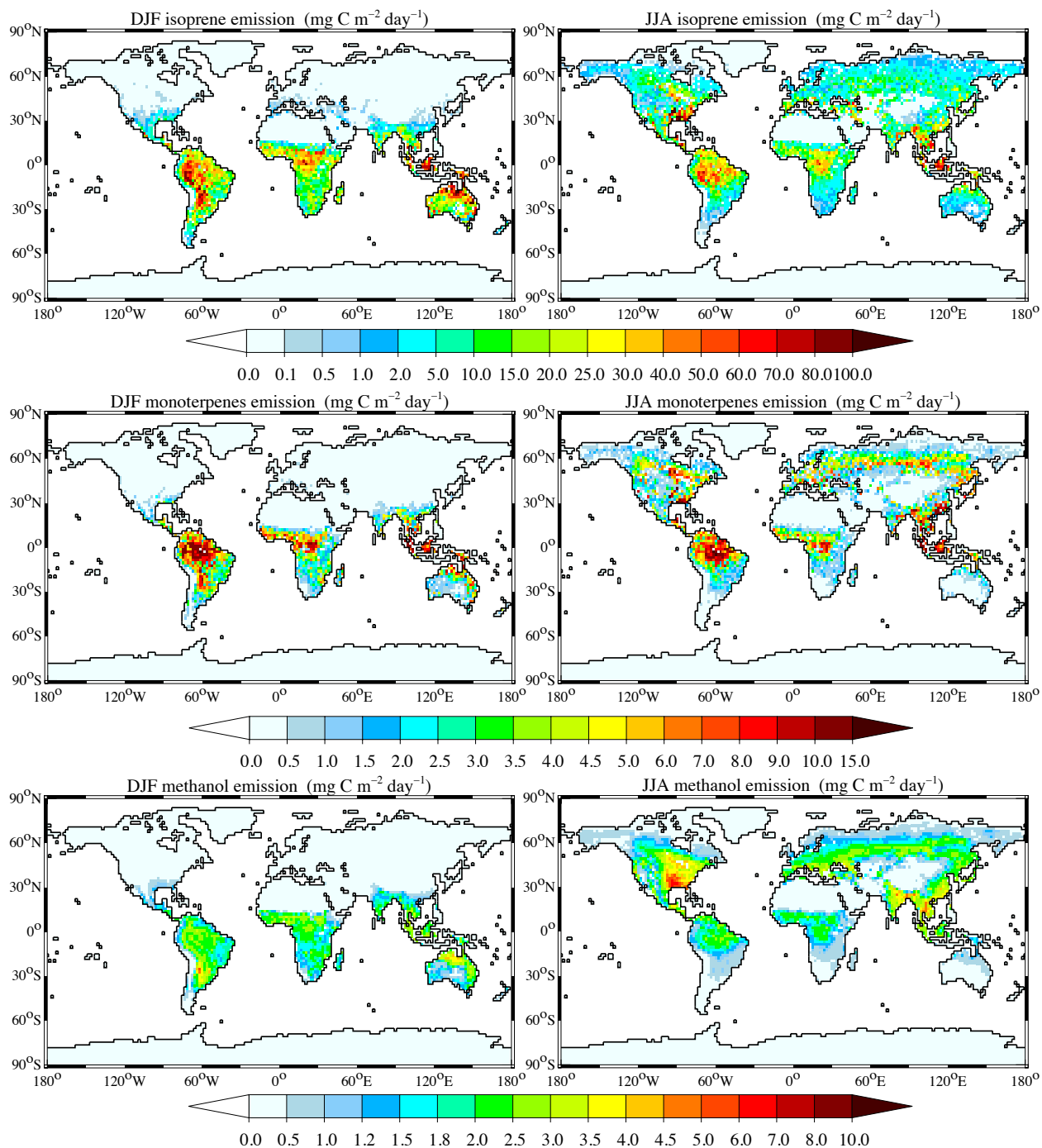
Figure 3. Spatial distribution of global December-January-February (DJF) and June-July-August (JJA) emissions (mg C m^{-2} day^{-1}) for isoprene, the sum of monoterpenes and methanol averaged over the 12 years (2000-2012) of the reference simulation.
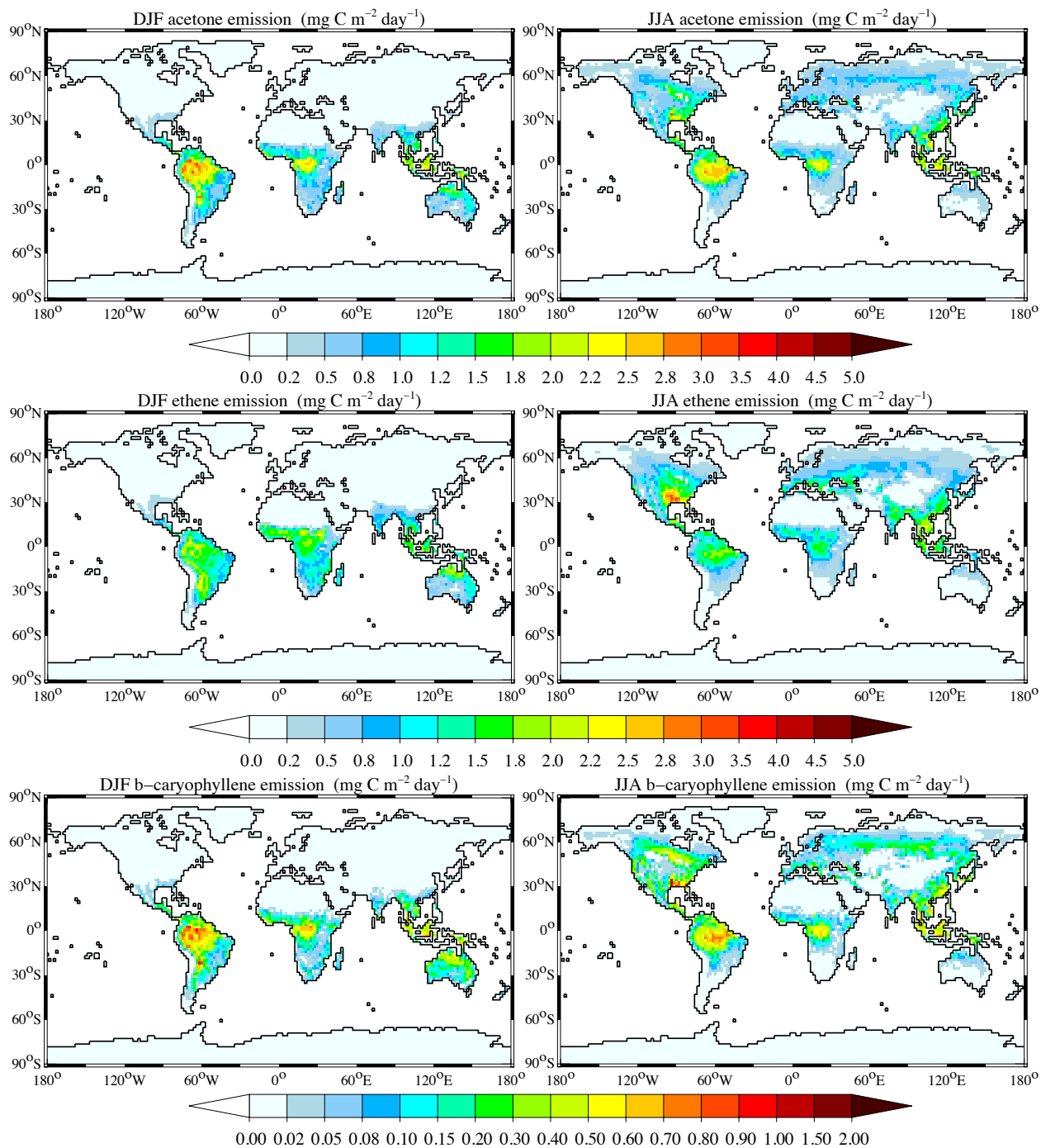
Figure 4. Same as Fig. 3 for acetone, ethene and β-caryophyllene.
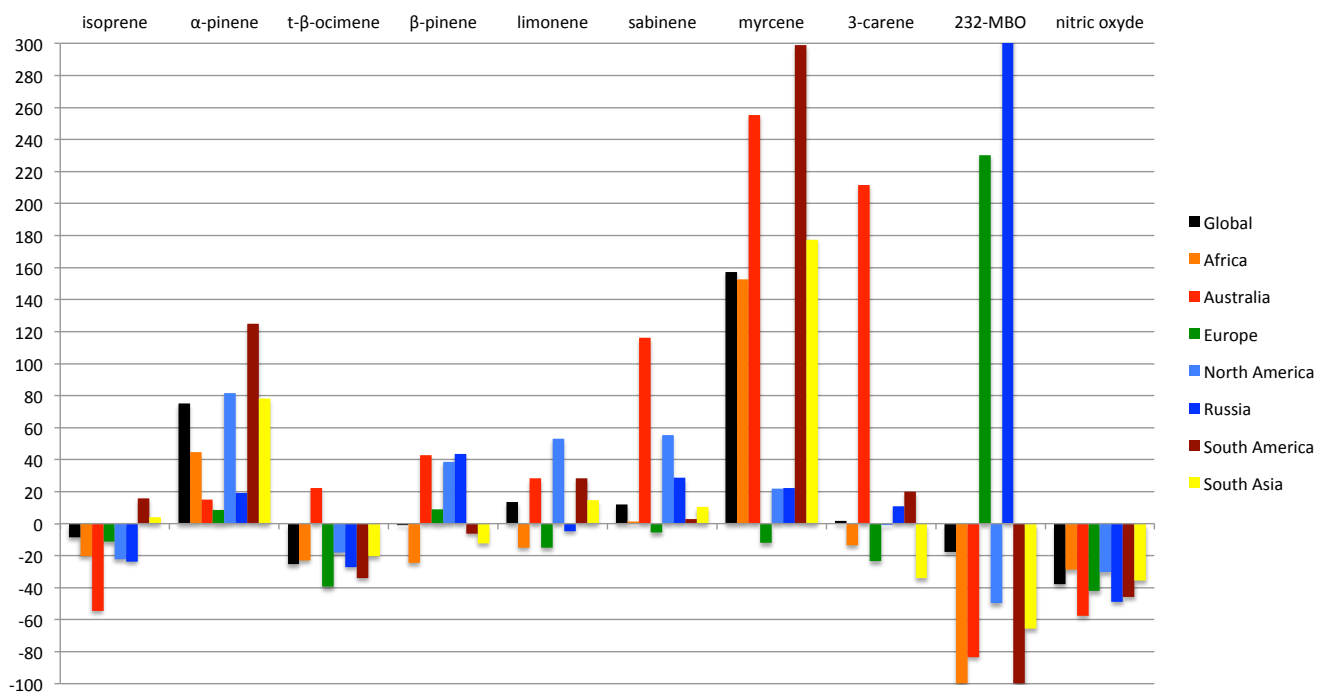
Figure 5. Global and regional relative emission differences (%) between the sensitivity simulation (PFT-CLM4) and the reference simulation for isoprene, monoterpenes, 232-MBO and nitric oxide.
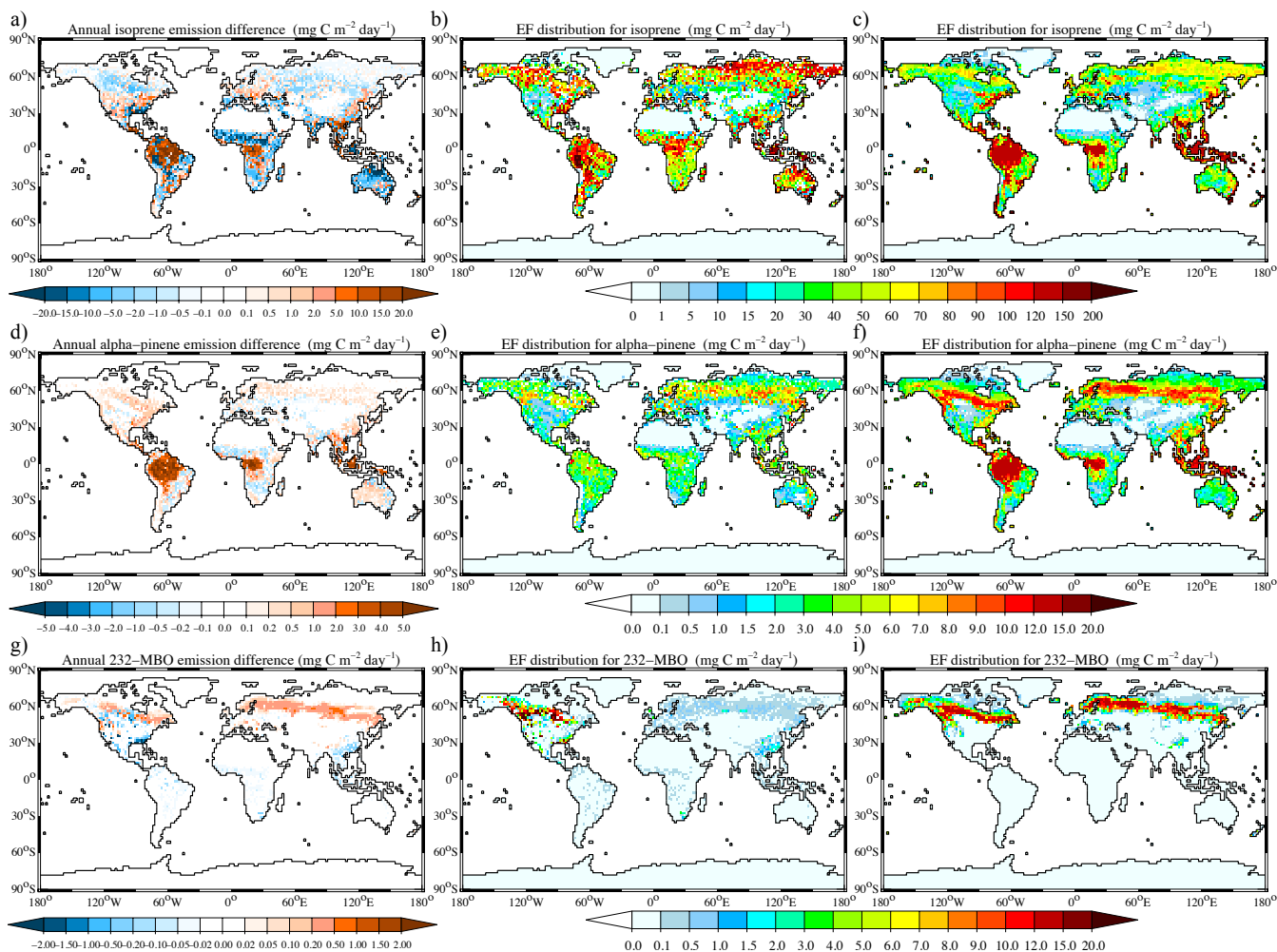
Figure 6. a) Difference in isoprene annual emissions (mg C m^{-2} day^{-1}) between the PFT-CLM4 and reference simulation, b) spatial distribution of emission factors (mg C m^{-2} day^{-1}) derived from global maps for isoprene , c) spatial distribution of emission factors (mg C m^{-2} day^{-1}) derived from MEGAN-CLM4 PFT distributions for isoprene; d), e), f) same as a), b), c) for α-pinene; g), h), i) same as a), b),c) for 232-MBO.
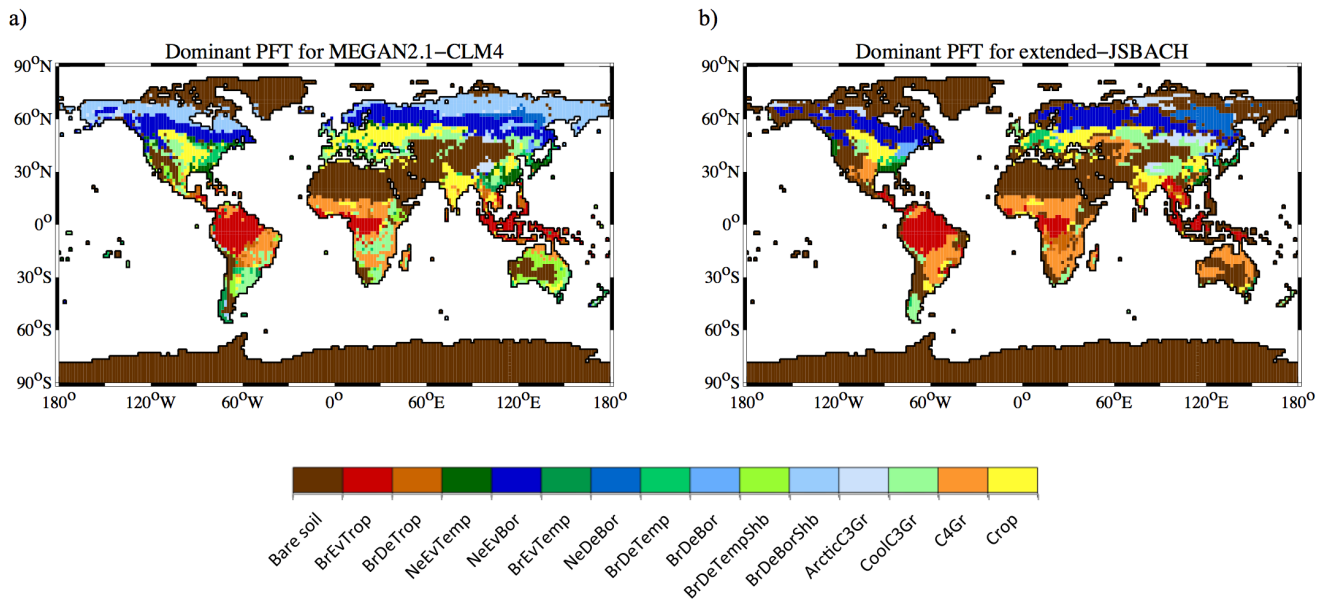
Figure 7. Distribution of dominant PFTs for a) MEGAN2.1-CLM4 and b) extended-JSBACH classifications.
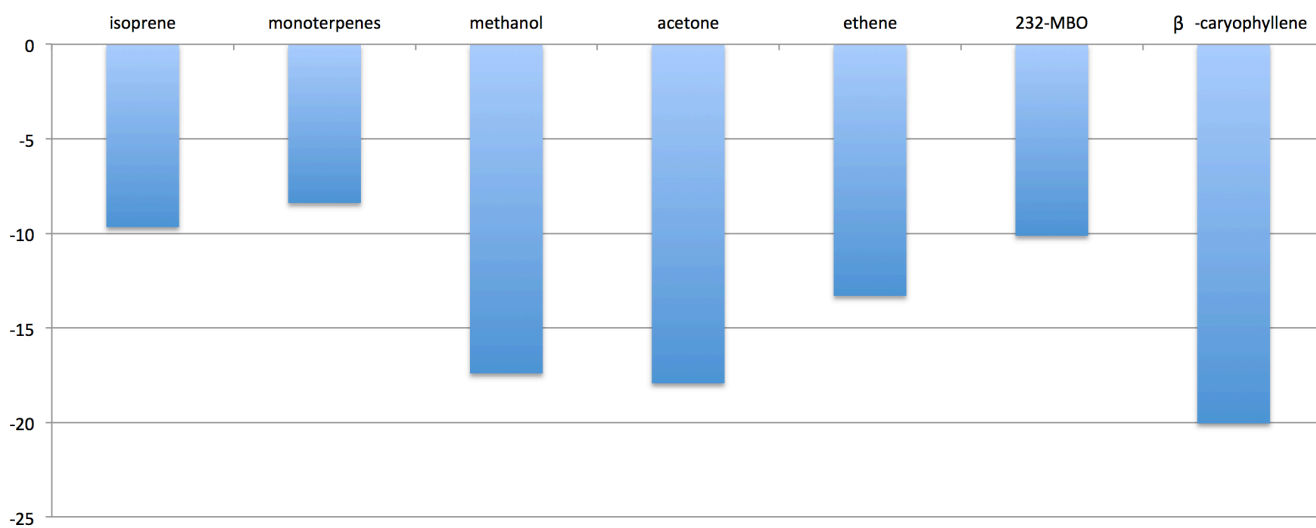
Figure 8. Global relative emission differences (%) between the sensitivity simulations PFT-JSBACH and PFT-CLM4 for isoprene, monoterpenes, methanol, acetone, ethene, 232-MBO and β-caryophyllene.
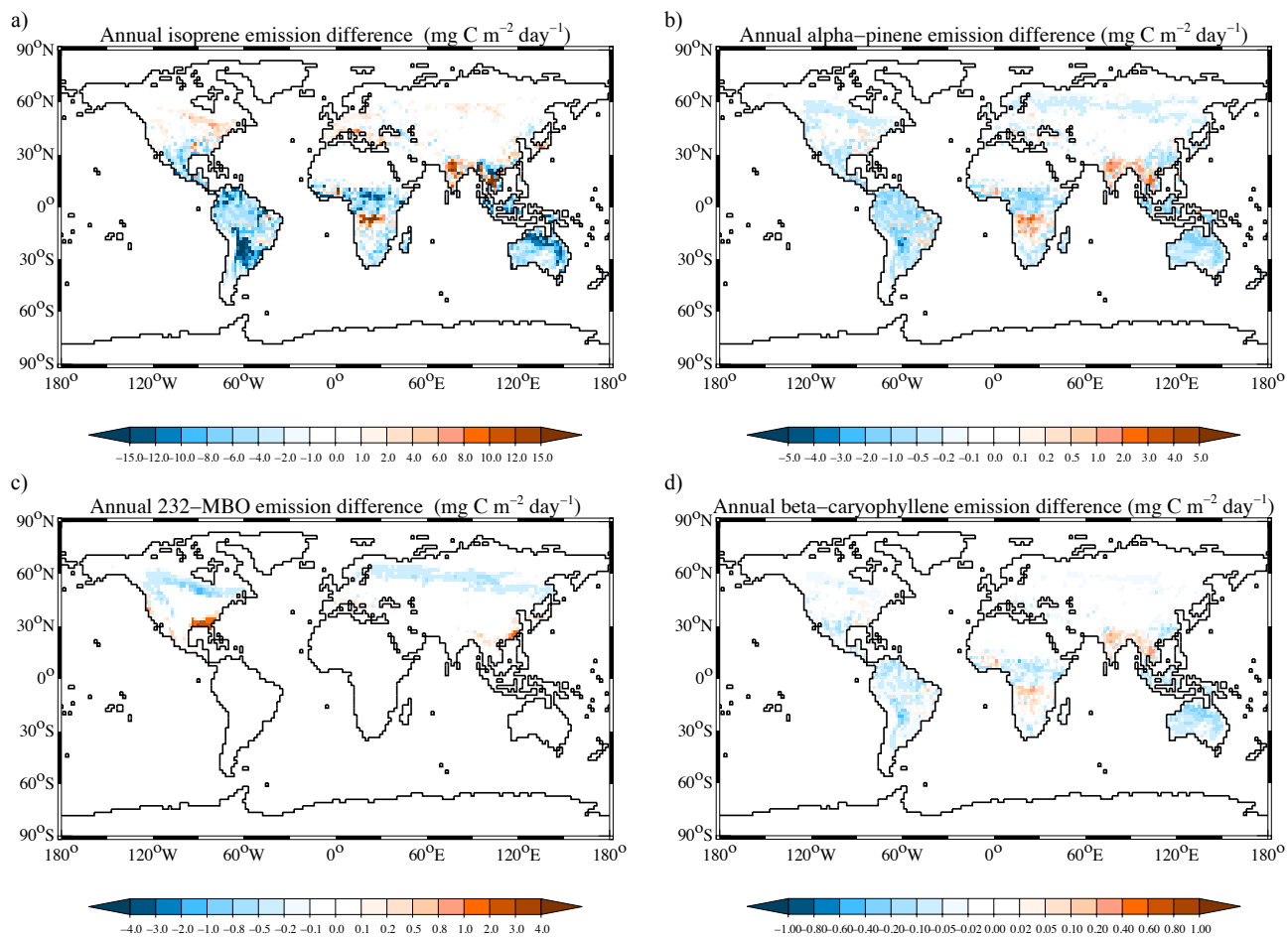
Figure 9. Difference in annual emissions (mg C m^{-2} day^{-1}) between the PFT-JSBACH ad PFT-CLM4 simulations for a) isoprene, b) α-pinene, c) 232-MBO, and d) β-caryophyllene.
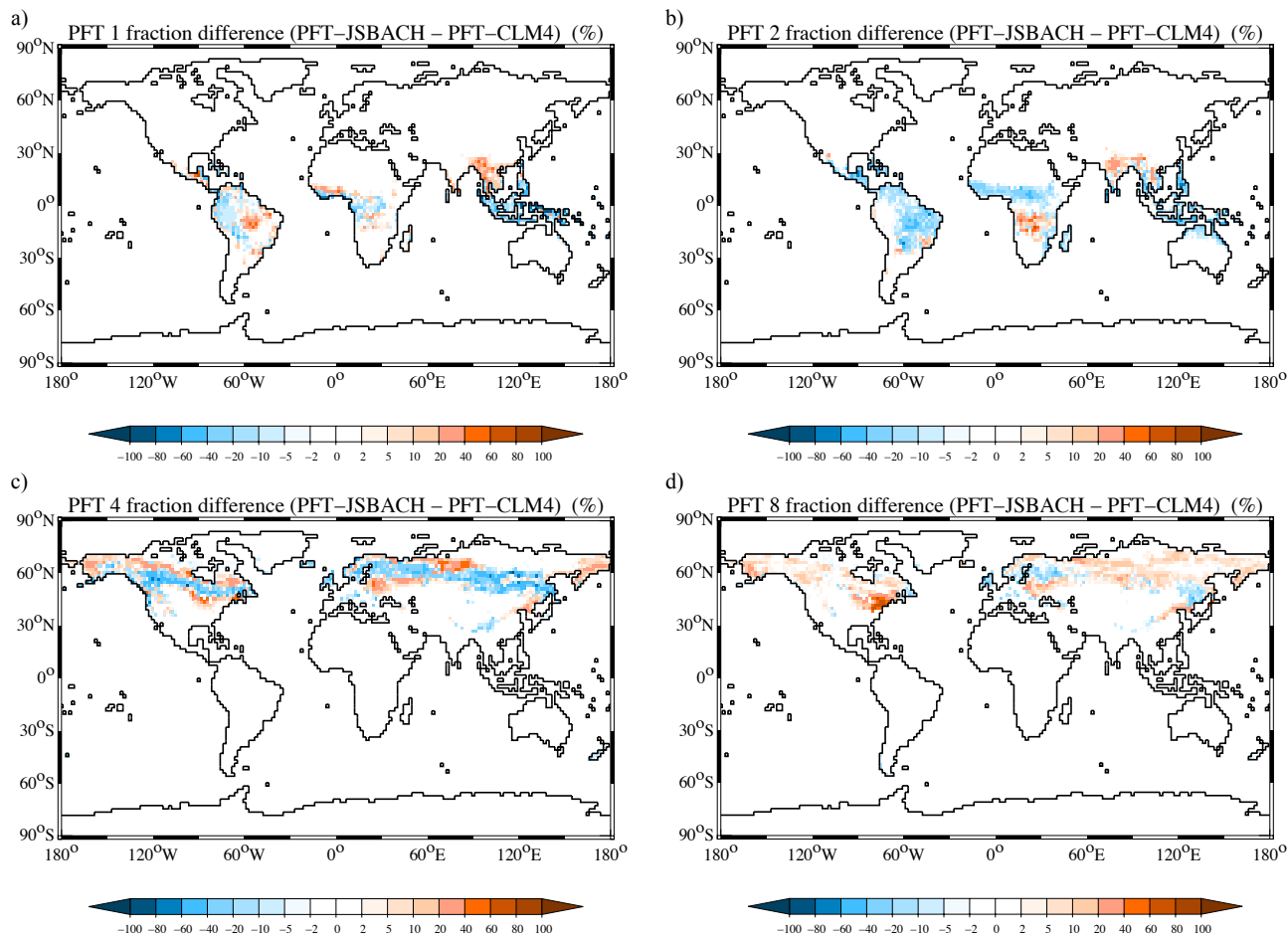
Figure 10. Difference between the extended-JSBACH PFT and the corresponding MEGAN2.1-CLM4 PFT distributions (cover fraction in %) for a) Broadleaf Evergreen Tropical trees, b) Broadleaf Deciduous Tropical trees, c) Needleleaf Evergreen Boreal Trees, and d) Broadleaf Deciduous Boreal Trees.
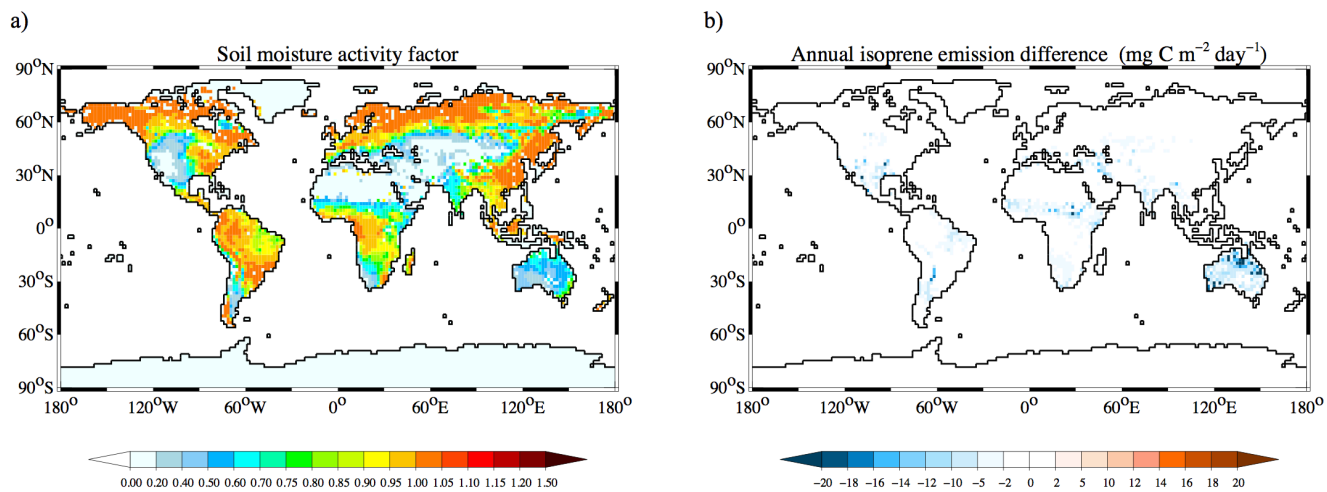
Figure 11. a) Annual soil moisture activity factor averaged over the simulation period, and b) annual isoprene emission differences (TEST-SM minus reference simulation) (Tg C year^{-1}).
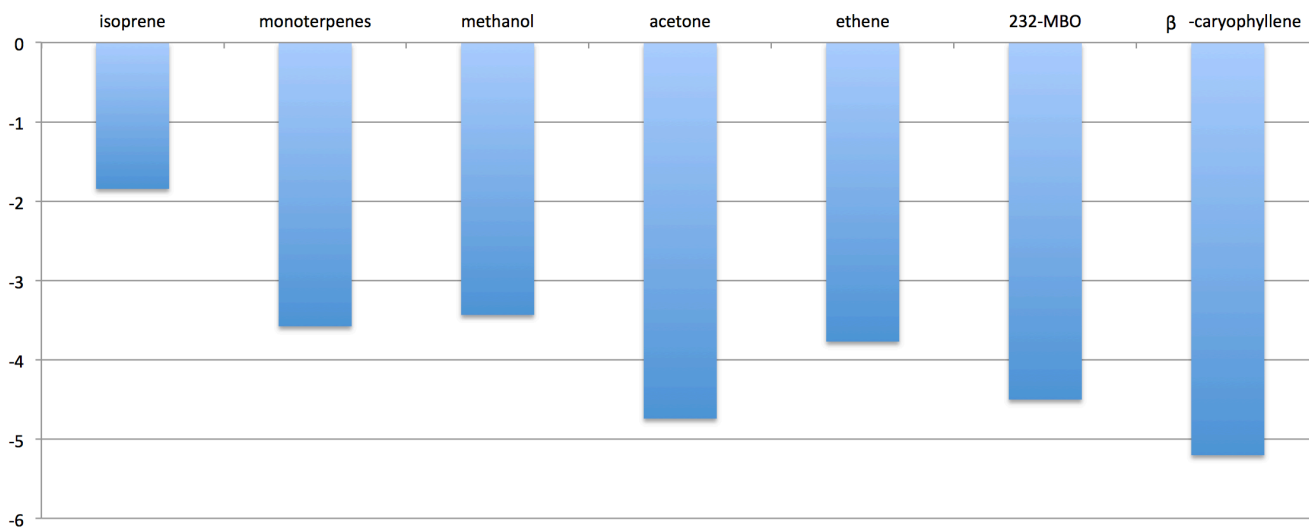
Figure 12. Global relative emission differences (%) between the sensitivity simulations TEST-NUDG and the reference simulation for isoprene, monoterpenes, methanol, acetone, ethene, 232-MBO and β-caryophyllene.
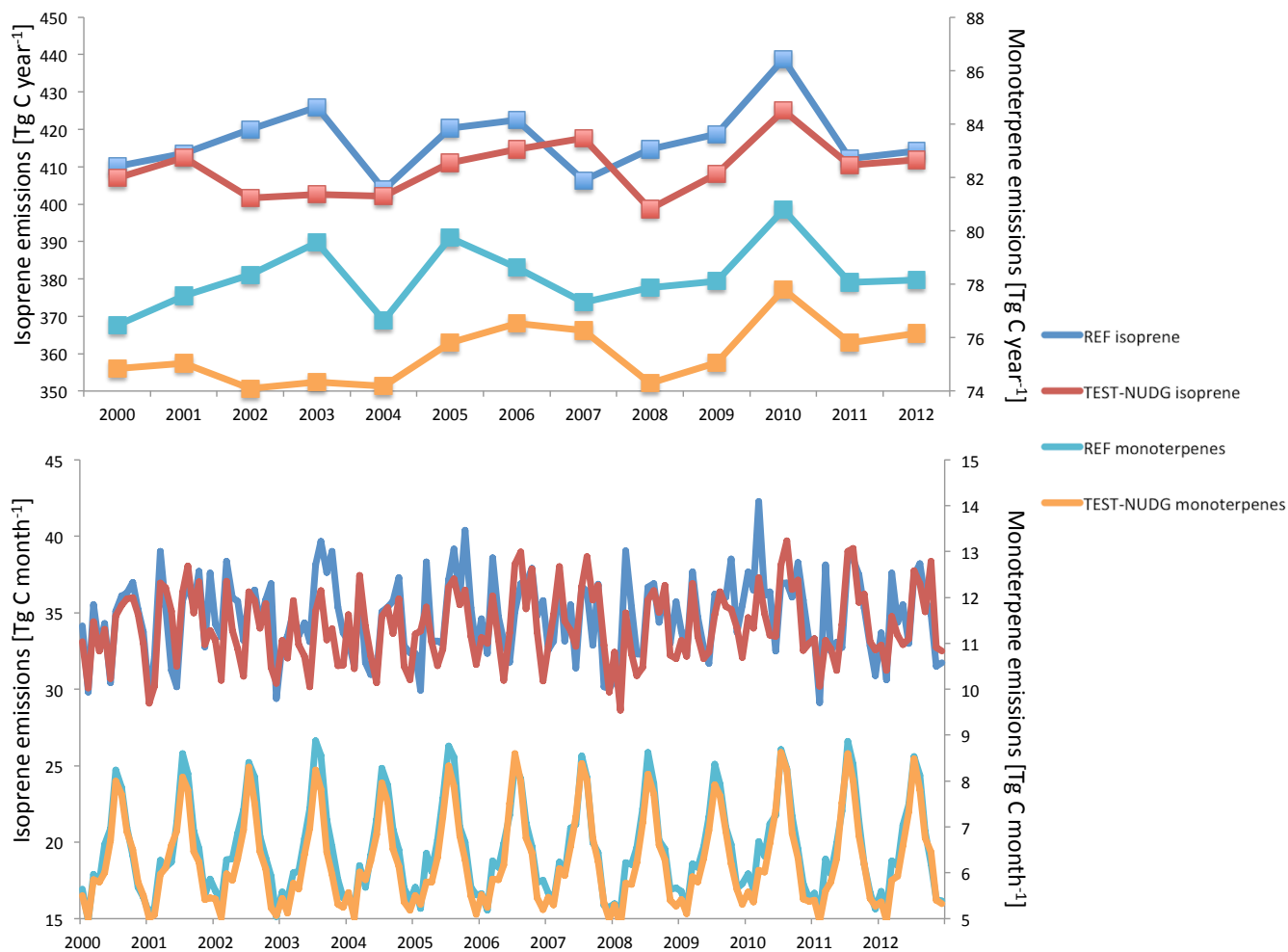
Figure 13. Temporal profiles of isoprene and monoterpenes global annual emissions (Tg C year^{-1}) (upper panel) and global monthly emissions (Tg C month^{-1}) (bottom panel) for the simulated 2000-2012 period.
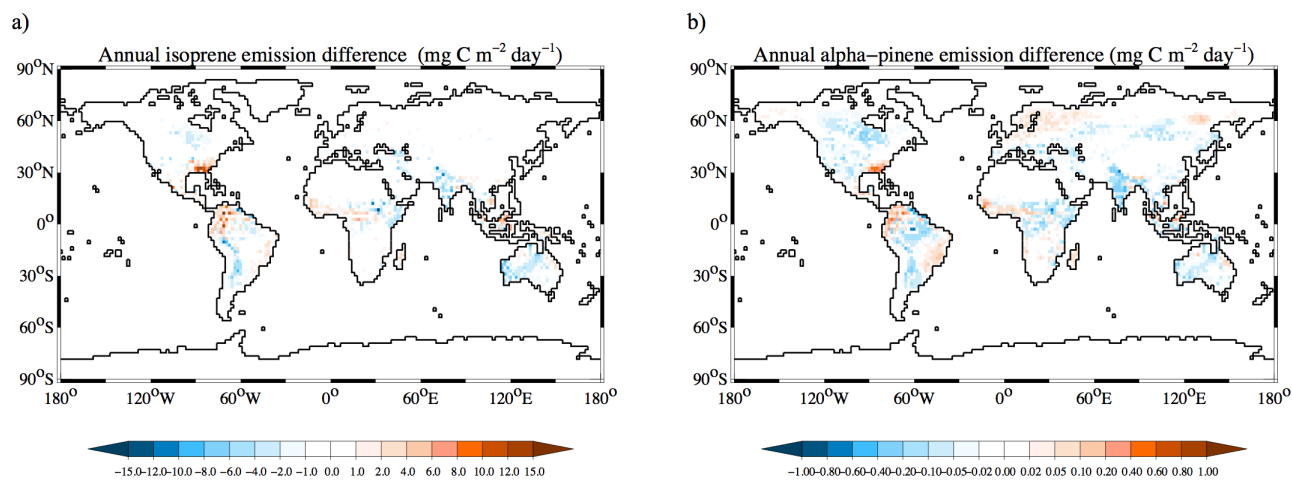
Figure 14. a) annual isoprene emission differences (TEST-NUDG minus reference simulation), and b) annual α-pinene emission differences (TEST-NUDG minus reference simulation).
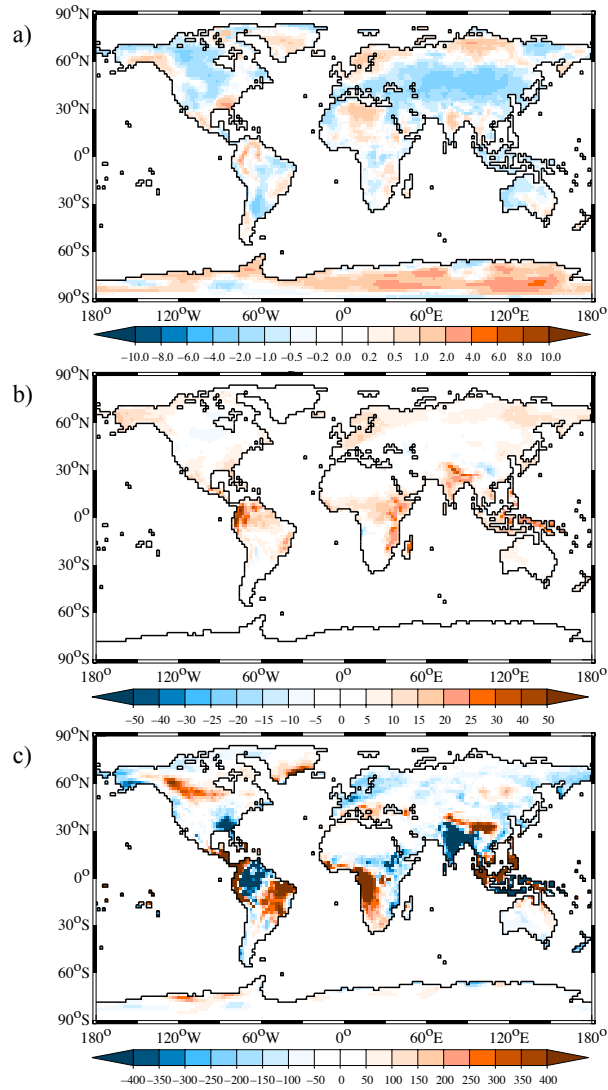
Figure 15. a) annual surface air temperature (°C), b) annual surface incoming shortwave radiation (W m^{-2}), and c) annual total precipitation (mm yr^{-1}) differences (TEST-NUDG minus reference simulation).